

FIG. 1. Structure of AK602.

MATERIALS AND METHODS

Transplantation of human PBMC in NOG mice. NOD-SCID (NOG) mice (10, 33) were maintained in the Central Institute for Experimental Animals (Kawasaki, Japan). Mice were 4 to 6 weeks old at the time of transfer of human PBMC. The human PBMC-transplanted NOG (hu-PBMC-NOG) mice were generated by methods previously described (23, 24). Briefly, PBMC (10^7) were freshly prepared from heparinized blood of a single healthy HIV-1-seronegative donor by Ficoll-Hypaque density gradient centrifugation, resuspended in RPMI 1640-based culture medium (0.5 ml), and infused intraperitoneally to each mouse. The experimental protocol was approved by the Ethics Review Committees for Animal Experimentation of the participating institutions.

Assay for proliferation and CCR5 expression of transplanted human PBMC recovered from hu-PBMC-NOG mice. Freshly isolated human PBMC (2×10^7 cells/ml) were incubated in phosphate-buffered saline (PBS) containing $10 \mu\text{M}$ 5-carboxyfluorescein diacetate succinimidyl ester (CFSE; Molecular Probes, Eugene, Oreg.) for 15 min at 37°C for CFSE labeling as previously described by Lyons (16), washed, and resuspended in RPMI 1640. One part of the labeled PBMC preparation was intraperitoneally injected (10^7 PBMC) to each NOG mouse, and human PBMC were recovered from peritoneal lavages and spleen. The other part of the preparation was immediately stimulated with $10 \mu\text{g}$ of phytohemagglutinin (PHA)/ml, cultured, and harvested. PBMC samples thus obtained were labeled with phycoerythrin (PE)-conjugated anti-CCR5 monoclonal antibody 3A9 or peridinin chlorophyll protein-conjugated anti-HLA-DR antibody (BD Pharmingen, San Diego, Calif.) and subjected to flow cytometric analysis with a Becton Dickinson FACScan cytometer; the data were analyzed by Cell Quest software (Becton Dickinson, Franklin Lakes, N.J.). A quantitative fluorescence-activated cell sorting (FACS) assay that relies on a series of precalibrated beads that bind to a fixed number of mouse immunoglobulin G molecules (Quantum Simply Cellular Kit; Sigma, Saint Louis, Mo.) to determine the absolute number of CCR5s on the cell surface was also conducted according to the manufacturer's instructions (15).

Cells and viruses. The HeLa-CD4-LTR- β -gal indicator cell line expressing human CCR5 (CCR5⁺ MAG1) (18), a kind gift from Yosuke Maeda, was used for the present study. 293T cells (a human embryonic kidney cell line) were cultured in Dulbecco's modified Eagle medium supplemented with 10% fetal calf serum (FCS) and antibiotics and used for transfection of DNA plasmid containing the R5 HIV-1_{JR-FL} genome (13). PBMC isolated from HIV-1-seronegative individuals were cultured with 10% FCS and antibiotics with $10 \mu\text{g}$ of PHA/ml for 3 days prior to anti-HIV-1 activity assay in vitro (PHA-PBMC). A panel of HIV-1 strains was employed for the drug susceptibility attempt: HIV-1_{Ba-L} (7), HIV-1_{JR-FL} (13), HIV-1_{NL4-3} (32), a wild-type HIV-1_{MORW} isolated from a drug-naive AIDS patient (17), and MDR primary HIV-1 (HIV-1_{MDR}) strain (HIV-1_{JSL} and HIV-1_{MM}) (35). All primary HIV-1 strains were passaged once or twice in PHA-PBMC cultures and the culture supernatants were stored at -80°C until use. Antiviral assays using PHA-PBMC were conducted as previously reported (12, 17, 35).

Antiviral agents and assay for inhibition of R5 HIV-1 infectivity and replication. A series of different spirodiketopiperazine (SDP) derivatives were newly designed, synthesized, and tested for their activity against in vitro infectivity and replication of R5 HIV-1 as previously described (17). AK602 was chosen for this study based on its CCR5-specific, potent activity against R5 HIV-1. A method for the synthesis of AK602 will be published elsewhere. The structure of AK602 is illustrated in Fig. 1. An approved drug for therapy for HIV-1 infection, 2',3'-dideoxinosine (ddI) (20, 21), was kindly provided by Ajinomoto Co., Inc, Tokyo, Japan. TAK779 and SCH-C were synthesized according to previously published data (1, 30). The MAG1 assay using CCR5⁺ MAG1 cells was conducted as previously described (17) with minor modifications. Briefly, CCR5⁺ MAG1 cells were seeded in 96-well, flat-bottomed microculture plates (10^4 cells/well) for 24 h, exposed to 0.1 or $1 \mu\text{M}$ AK602 for 30 min, washed three times, exposed to

R5 HIV-1 (100 50% tissue culture infectious doses) at various time points after AK602 removal, and cultured in Dulbecco's modified Eagle medium containing 15% FCS for 48 h. Following the removal of supernatants and lysis of the cells with PBS (100 μl) containing 1% Triton X-100, a solution (100 μl) containing 10 mM chlorophenol red- β -D-galactopyranoside, 2 mM MgCl_2 , and 0.1 M KH_2PO_4 was added to each well; the mixture was incubated at room temperature in the dark for 30 min; and the optical density (wavelength, 570 nm) was measured with a microplate reader (Vmax, Molecular Devices, Sunnyvale, Calif). All assays were performed in triplicate.

Pharmacokinetic analysis of AK602 in hu-PBMC-NOG mice. Pharmacokinetic analysis of AK602 in hu-PBMC-NOG mice was performed as previously described (28). In brief, plasma samples were collected periodically over 12 h, following a single AK602 administration at a dose of 60 mg/kg of body weight dissolved in 400 μl of 4% hydroxypropyl- β cyclodextrin (HPBC). Each plasma sample (150 μl) was centrifuged at 3,000 rpm for 10 min, and the supernatant was vacuum concentrated and injected into the high-performance liquid chromatography (HPLC) system. The eluent was monitored at 255 nm of UV, and the AK602 concentration in plasma was determined.

Determination of amounts of AK602 persistently bound to CCR5 in hu-PBMC-NOG mice. Blood samples were collected from the tail vein of each hu-PBMC-NOG mouse at various time points following a single intraperitoneal administration of AK602 at a dose of 60 mg/kg. PBMC were isolated by density gradient centrifugation and stained with fluorescein isothiocyanate-conjugated monoclonal antibody 45531 (R&D Systems, Minneapolis, Minn.) specific for the C-terminal half of the second extracellular loop (ECL2B) of CCR5 (15) known to be competitively replaced by SDP derivatives (17) or with PE-conjugated monoclonal antibody 3A9, which binds to the N-terminus extracellular domain of CCR5 (17). PBMC were then subjected to FACS analysis.

Treatment of R5 HIV-1-infected hu-PBMC-NOG mice with anti-HIV-1 agents. Sixteen days after PBMC infusion, the mice were bled from the tail vein, and three-color flow cytometric analysis was performed to confirm positive engraftment of human HLA, CD4, and CD8 antigens on the cells recovered. HIV-1_{JR-FL} (2,000 50% tissue culture infectious doses) was intraperitoneally inoculated to each mouse in which PBMC engraftment was confirmed. Twenty-four hours after the R5 HIV-1 inoculation, administration of AK602 (120 mg in 4% HPBC/kg/day, twice a day), ddI (50 mg in 4% HPBC/kg/day, twice a day), or saline was implemented and continued by day 16. On days 5 and 9 after the R5 HIV-1 inoculation, blood samples were collected from mouse tail veins for immunologic and virological monitoring (see below). On day 16, blood samples were collected by cardiocentesis, and the mice were sacrificed. The experimental protocol for the treatment is illustrated in Fig. 2.

Immunologic and virological monitoring. Human PBMC recovered from mice were subjected to immunologic and virological monitoring as previously described (23, 24). The $\text{CD}4^+/\text{CD}8^+$ cell ratios were determined by FACS analysis with PE-conjugated mouse anti-CD4 and peridinin chlorophyll protein-conjugated mouse anti-CD8 (BD Pharmingen) monoclonal antibodies. Determination of HIV-1 DNA copy numbers in recovered human PBMC was performed by real-time PCR assay with Taqman Master mixture (PE Biosystems) and HIV long terminal repeat-specific primers M667 (5'-GGC TAA CTA GGG AAC CCA CTG-3') and AA55 (5'-CTG CTA GAG ATT TTC CAC ACT GAC-3'). HIV-1-specific products were quantified with the ABI 7700 detection system (Applied Biosystems, Foster City, Calif.), and cell numbers were determined with the RAG-1 gene. The numbers of $\text{CD}4^+$ cells were calculated based on the percentage of $\text{CD}4^+$ values obtained from the FACS analysis of each test PBMC sample, and R5 HIV-1 proviral DNA copy numbers were expressed as copy numbers per $10^5 \text{CD}4^+$ cells. In some experiments, $\text{CD}4^+$ and $\text{CD}4^-$ cells were separated before real-time PCR assay with the rapid immunomagnetic $\text{CD}4^+$ positive cell isolation kit (Dynabeads M-450 $\text{CD}4$; Dynal Biotech, Inc., Lake

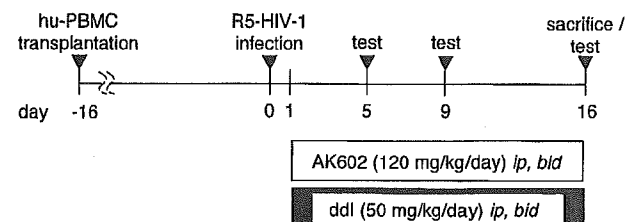


FIG. 2. Protocol for drug administration and immunological and virologic monitoring.

Success, N.Y.). The amounts of p24 antigen in murine sera were determined using a fully automated chemiluminescent enzyme immunoassay system (Lumipulse F; Fujirebio, Inc., Tokyo, Japan) as previously described (12). Plasma viral load was quantified with the AMPLICOR HIV-1 monitor test kit, version 1.5 (Roche Diagnostics, Branchburg, N.J.).

Statistical analyses. Nonparametric statistical analyses were performed by using the Mann-Whitney U test (Statview, version 5.0; Abacus Concepts, Berkeley, Calif.). The difference between viremia levels in two groups of mice was determined by the Wilcoxon rank sum test. For each mouse, the value of \log_{10} RNA copies was calculated, and the slope corresponding to the rate of increase per day was determined by simple linear regression for the days (5, 9, and 16) of blood collection. The resulting slopes for all mice in the untreated groups were compared to the slopes of mice in each of the other two groups.

RESULTS

Transplanted PBMC in hu-PBMC-NOG mice are intensely activated and express high levels of CCR5. When we examined the proliferation profile of PBMC stimulated with PHA *in vitro* by treatment with the vital dye CFSE, which allows the analysis of cell proliferation as the CFSE's fluorescence intensity is halved per each cell division, there was only a slight shift to the left in the flow cytometric profile on days 1 and 2 of culture (Fig. 3A). On day 4 of culture, a discrete shift to the left was identified, suggesting that the PHA-PBMC underwent up to four cycles of proliferation *in vitro* by day 4. In contrast, PBMC transplanted and recovered on day 2 had apparently undergone ~ 4 cycles of proliferation; by day 4, a majority of cells had undergone up to 10 cycles and beyond in proliferation (Fig. 3B). It was possible that the CFSE-negative and weakly CFSE-positive cells which accumulated on days 2 and 4 (Fig. 3B) were murine cells that engulfed and degraded CFSE. We therefore conducted experiments in which the cells with CFSE dilution were directly confirmed to be human CCR5-positive cells. As can be seen in Fig. 3C, when cells were recovered from the spleen of an NOG mouse into which CFSE-labeled PBMC had been transplanted and stained with monoclonal antibody 45531, which is specific for the C-terminal half of the second extracellular loop (ECL2B) of CCR5 (15), the majority of such human CCR5⁺ cells proved to be CFSE negative. We also examined the levels of cellular activation by the expression of HLA-DR on cell surface. The levels of HLA-DR expression in PBMC recovered from uninfected NOG mice 3 days after transplantation were much greater than those in 3-day-cultured PBMC following PHA stimulation (Fig. 3D). The fluorescence intensity in the same donor's PHA-PBMC examined on three different occasions was 21 ± 4 , while that of the PBMC recovered from mice was 91 ± 25 (Fig. 3D). When we further assessed the levels of CCR5 expression, the PBMC recovered from the mice on day 3 proved to be strongly positive for CCR5 (Fig. 3E). The CCR5-positive fraction in the PBMC recovered was 49.7%, while that in PHA-PBMC was 27.3%. The mean fluorescence intensity of the CCR5⁺ cell population was 141, compared to the CCR5⁺ cell population in PHA-PBMC with a mean fluorescence intensity of 51. The estimated number of CCR5 expressed on the PBMC recovered on day 3 was 25,348 (as antibody binding sites per cell) while that on PHA-PBMC on day 3 in culture was 8,981 antibody binding sites as examined by quantitative FACS assay. These data indicate that the transplanted human PBMC were intensely activated and rapidly proliferating and expressed high levels of CCR5 on their cell surfaces.

Potent activity of AK602 against R5 HIV-1 *in vitro*. Among SDP derivatives we designed and synthesized, AK602 was identified to be highly potent against a broad spectrum of R5 HIV-1 strains, including MDR clinical R5 HIV-1 isolates *in vitro* with 50% inhibitory concentration (IC_{50}) values of 0.3 to 0.6 nM, although two previously published CCR5 antagonists (TAK779 and SCH-C) were substantially less potent than AK602 (Table 1). AK602 and other CCR5 antagonists failed to inhibit the replication of an X4 HIV-1 strain, HIV-1_{NL4-3}.

Pharmacokinetics of AK602 in hu-PBMC-NOG mice. We examined the pharmacokinetics of AK602 in hu-PBMC-NOG mice by intraperitoneally administering the compound at a dose of 60 mg/kg. Plasma samples were collected periodically up to 12 h and subjected to HPLC analysis. As shown in Fig. 4A, the concentration of AK602 reached the maximal concentration immediately after intraperitoneal administration and decreased rapidly. The calculated plasma half-life in the α -phase of the concentration curve was as short as 29 min.

AK602 persists on cell surface CCR5. As shown above, the plasma half-life of AK602 turned out to be short; however, considering that AK602 possesses such a high affinity to CCR5 and potent activity against R5 HIV-1 *in vitro*, it was thought possible that AK602 would remain attached on cellular CCR5 for an extensive period of time and exert anti-R5 HIV-1 activity even when the compound was depleted from circulation. To examine this possibility, we used two monoclonal antibodies, 45531 and 3A9. When human PBMC were recovered from a hu-PBMC-NOG mouse 2 and 6 h after AK602 administration (60 mg/kg) and stained with 45531, AK602 proved to block the binding of 45531 to CCR5 (Fig. 4B), while AK602 failed to block 3A9 binding to CCR5 (Fig. 4C), suggesting that AK602 did not elicit CCR5 internalization or shedding at all at least for 6 h. We subsequently examined whether AK602 remained on cellular CCR5 with the 45531 monoclonal antibody. When the cells were recovered from mice 2, 6, and 14 h after the AK602 administration, the mean values of the percentage of AK602 occupancy were 85 (four mice), 54 (three mice), and 16 (three mice), respectively. It was calculated that it took about 9 h for AK602 occupancy to be reduced by 50% (Fig. 4D).

Anti-R5 HIV-1 activity of AK602 persistently seen after its removal from culture medium. In another depletion experiment, we exposed CCR5⁺ MAGI cells to AK602 for 30 min, depleted the compound from the culture by thorough washing, incubated the cells for various lengths of time, exposed the cells to HIV-1_{Ba-L}, further cultured the cells for 48 h, and determined whether HIV-1_{Ba-L} infection was blocked by AK602 exposure (Fig. 4E). When the CCR5⁺ MAGI cells were exposed to 0.1 and 1 μ M AK602 and exposed to HIV-1_{Ba-L} immediately afterward, the values for protection were 68 and 85%, respectively. When the cells were exposed to HIV-1_{Ba-L} 4 h after depletion, 49 and 72% of the cells were protected by 0.1 and 1 μ M AK602. When the cells were exposed to HIV-1_{Ba-L} 12 and 24 h after depletion, 57 and 45% of the cells were seen protected by 1 μ M, respectively (Fig. 4E).

Effects of AK602 on CD4⁺ and CD8⁺ cell counts in R5 HIV-1-infected hu-PBMC-NOG mice. PBMC were recovered from murine blood samples collected on days 5, 9, and 16 after R5 HIV-1 inoculation and subjected to flow cytometric analysis for determination of CD4⁺/CD8⁺ cell ratios. As shown in Fig. 5A, in PBMC recovered on day 16 from a representative

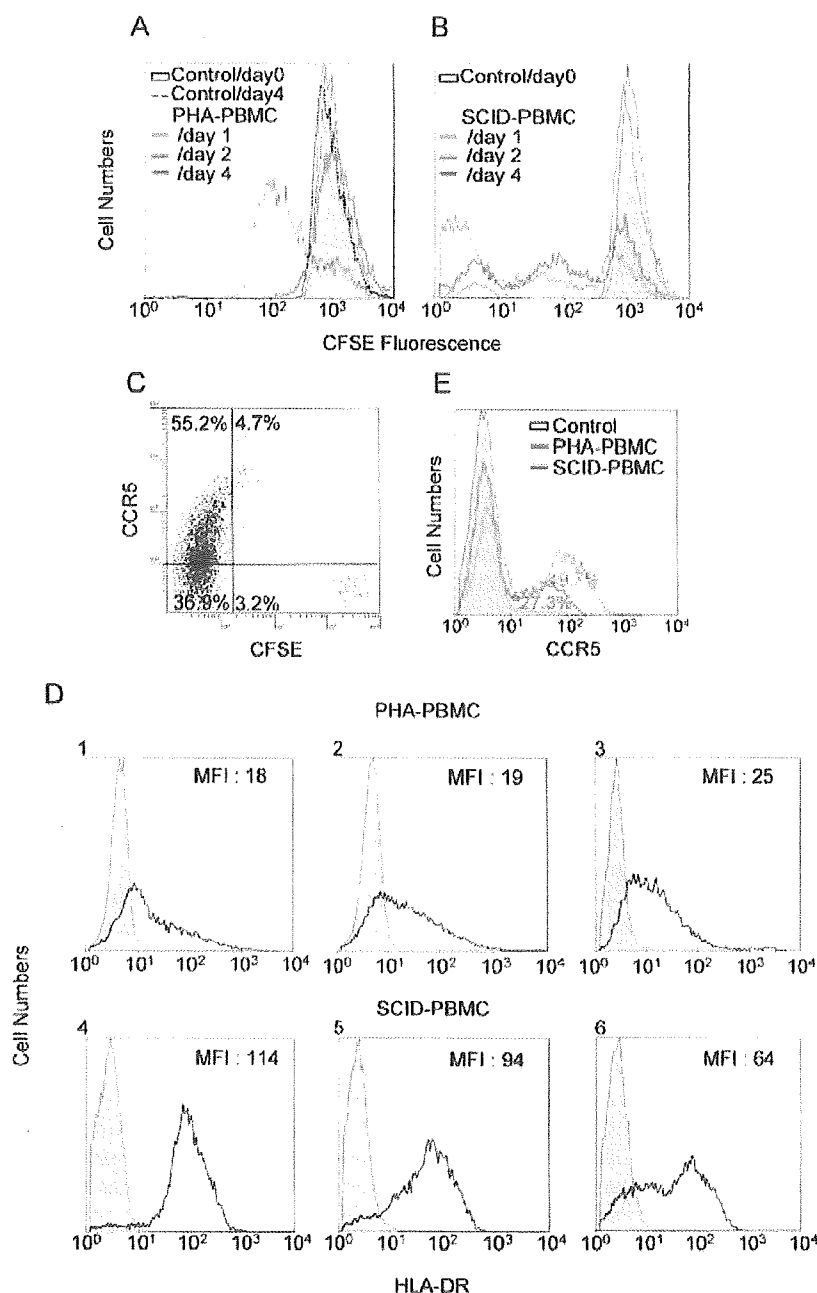


FIG. 3. Transplanted PBMC are intensely activated and express high levels of CCR5. (A and B) Proliferation profiles of PHA-PBMC and transplanted and recovered PBMC. Freshly prepared PBMC were incubated with the vital dye CFSE, and one part of such PBMC preparation was stimulated with PHA, while the other part was intraperitoneally transplanted to mice. On days 1, 2, and 4, the cells were harvested and the fluorescence intensity of CFSE was determined. Note that transplanted PBMC recovered on day 2 had undergone ~4 cycles of proliferation; by day 4, a majority of cells had undergone ~10 cycles and more of proliferation. (C) CCR5 expression level and CFSE intensity in human PBMC harvested from a spleen of hu-PBMC-NOG mouse on day 4. (D) Intense activation of PBMC after transplantation. PBMC stimulated with PHA and cultured for 4 days (panels 1 to 3) and transplanted PBMC recovered from the uninfected mice on day 4 (panels 4 to 6) were stained with an anti-HLA-DR monoclonal antibody. Note that HLA-DR expression levels in transplanted PBMC were much higher than those in PHA-PBMC. (E) CCR5 expression profiles of PHA-PBMC and transplanted PBMC. PBMC stimulated with PHA and cultured for 3 days and transplanted PBMC recovered from the uninfected mice on day 3 were stained with PE-conjugated anti-CCR5 monoclonal antibody 3A9 and subjected to flow cytometric analysis. SCID-PBMC, PBMC transplanted and recovered.

R5 HIV-1-infected, saline-treated mouse, there were only few CD4⁺ cells (3.9% [1.4% + 2.5%]) resulting in a CD4⁺/CD8⁺ cell ratio of 0.05. However, a distinct CD4⁺ cell population (55.1% [4.4% + 50.7%]) resulting in a CD4⁺/CD8⁺ ratio of

1.84 (Fig. 5B) was seen in PBMC recovered from an AK602-treated mouse, and the size of this CD4⁺ cell population was comparable to that seen in a ddI-treated mouse (53.2% [3.8% + 49.4%]) and that in an uninfected mouse (48.9% [3.8% +

TABLE 1. Anti HIV-1 activity of novel SDP derivatives in PBMC^a

Compound	IC ₅₀ value in p24 assay (nM)					
	HIV-1 _{Ba-L} (R5)	HIV-1 _{JRFL} (R5)	HIV-1 _{MOKW} (R5)	HIV-1 _{MM} (R5 _{MDR})	HIV-1 _{JSL} (R5 _{MDR})	HIV-1 _{NL4-3} (X4)
AK602	0.5 ± 0.3	0.2 ± 0.1	0.3 ± 0.2	0.7 ± 0.3	0.4 ± 0.2	>1,000
TAK779	14 ± 5	6 ± 2	9 ± 3	12 ± 4	10 ± 3	>1,000
SCH-C	3 ± 2	2 ± 1	2 ± 1.5	2.5 ± 1	2 ± 1	>1,000
ZDV	13 ± 5	7 ± 3	10 ± 6	520 ± 75	64 ± 13	9 ± 5
SQV	8 ± 3	6 ± 2	6 ± 3	212 ± 56	276 ± 44	10 ± 4

^a IC₅₀s were determined by using PHA-PBMC isolated from three different donors, and the inhibition of p24 Gag protein production was used as an endpoint. All assays were conducted in triplicate. The results shown represent arithmetic means (±1 standard deviation) of three independently conducted assays. HIV-1_{MOKW} was isolated from a drug-naïve AIDS patient, and HIV-1_{JSL} and HIV-1_{MM} were isolated from patients who received antiretroviral therapy for a long period of time and whose virus loads showed a number of RT and PR mutations. Two previously published CCR5 inhibitors, TAK779 and SCH-C, and zidovudine (ZDV) and saquinavir (SQV) were used as reference compounds.

45.1%]), resulting in the ratios of 1.43 and 1.40 (Fig. 5C and D), respectively. Figure 6A illustrates the overall profiles of CD4⁺/CD8⁺ cells ratios on day 16 in the four groups. The mean CD4⁺/CD8⁺ cell ratio in mice (*n* = 7) given saline was 0.1 (range, 0.06 to 0.20). In contrast, the ratios in AK602-

treated mice (*n* = 8) were significantly higher with a mean value of 0.92 (range, 0.23 to 1.89; *P* = 0.001), which was comparable to that in ddI-treated mice (*n* = 9; mean, 1.29; range, 0.38 to 2.68; *P* = 0.001) and uninfected mice (*n* = 7; mean, 1.0; range, 0.50 to 1.49). The numbers of CD4⁺ cells/μl

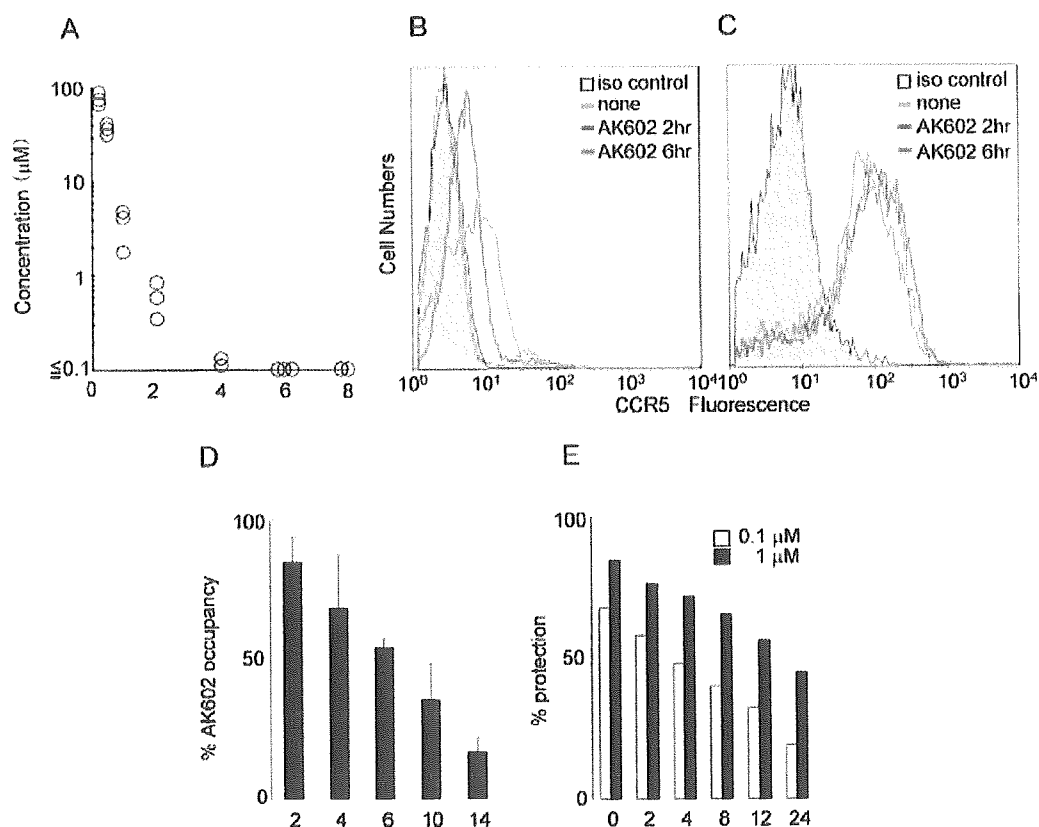


FIG. 4. Pharmacokinetics and persistence of anti-HIV-1 activity of AK602. (A) Pharmacokinetics of AK602. Each mouse was administered AK602 at a dose of 60 mg/kg, and blood samples were taken at 15, 30, 60, 120, 240, 480, and 720 min. Plasma concentrations of AK602 determined by HPLC analysis at 15, 30, 60, 120, and 240 min were 76.2, 36.1, 3.5, 0.6, and 0.13 μM, respectively. AK602 was not detected at later time points. (B and C) No CCR5 internalization or shedding was caused by AK602. Human PBMC were recovered 2 and 6 h after AK602 administration and stained with 45531 (B) or 3A9 (C). (D) Sustained AK602 occupancy on cell surfaces. At indicated periods of time after a bolus of AK-602 (60 mg/kg) was administered to hu-PBMC-NOG mice, PBMC were recovered and the percentages of AK602 occupancy on cellular CCR5 were determined with fluorescein isothiocyanate-conjugated monoclonal antibody 45531. (E) Persistence of in vitro activity of AK602 against R5 HIV-1 after AK602 depletion. CCR5⁺ MAGI cells were exposed to 0.1 or 1 μM AK602 for 30 min and thoroughly washed to deplete AK602 from the medium. The cells were subsequently cultured for the indicated periods of time, exposed to HIV-1_{Ba-L}, and further cultured for 48 h, when the cells were harvested and lysed with Triton X-100-containing PBS. A solution containing chlorophenol red-β-D-galactopyranoside was added, the optical density was measured, and the percentage of protection was determined.

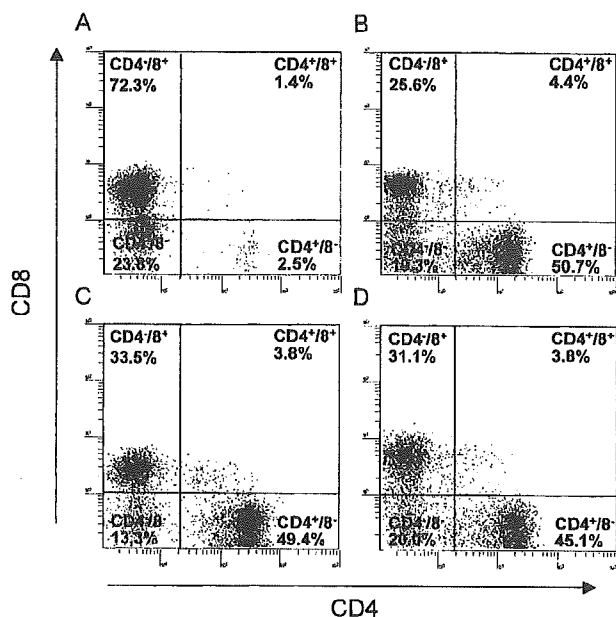


FIG. 5. Effects of AK602 on CD4⁺ and CD8⁺ cell counts in infected hu-PBMC-NOG mice. PBMC recovered on day 16 after R5 HIV-1 inoculation were subjected to flow cytometry. Shown are representative flow cytometric analysis profiles. Note that only 3.9% of CD4⁺ cells were seen (A), resulting in a CD4⁺/CD8⁺ cell ratio of 0.05 in a mouse given saline, while distinct numbers of CD4⁺ cells (55.1 and 53.2%) (B and C) were seen in AK602- and ddI-administered infected mice, resulting in CD4⁺/CD8⁺ cell ratios of 1.84 and 1.43, respectively. In an uninfected mouse (D), 48.9% of cells were positive for CD4, with a CD4⁺/CD8⁺ cell ratio of 1.40.

in saline-treated mice were significantly less than those of AK602-treated, ddI-treated, or uninfected mice (Fig. 6B).

Effects of AK602 on R5 HIV-1 proviral DNA copy numbers and serum p24 levels in R5 HIV-1-infected hu-PBMC-NOG mice. We next asked which population harbored proviral DNA in the cells recovered from R5 HIV-1-infected hu-PBMC-NOG mice, by purifying CD4⁺ and CD4⁻ cell populations and determining proviral DNA copy numbers in each population. As shown in Table 2, more than 99% of proviral DNA was found in CD4⁺ cells and <0.3% of proviral DNA was detected in CD4⁻ cells derived from saline-treated mice, indicating that R5 HIV-1 infection occurred in CD4⁺ cells in the hu-PBMC-transplanted NOG environment. As illustrated in Fig. 6C, the mean number of R5 HIV-1 proviral DNA copies was 2.0×10^5 (range, 2.6×10^4 to 1.7×10^6) per 10^5 CD4⁺ cells in R5 HIV-1-infected mice ($n = 7$) given saline. However, values for mice in groups given AK602 and ddI were 1.3×10^3 (range, 2.3×10^2 to 7.9×10^3 ; $P = 0.001$) and 1.8×10^2 (range, $<10^2$ to 7.9×10^2 ; $P = 0.001$), respectively.

The amounts of R5 HIV-1 p24 in serum were also found to be very high in saline-treated mice, with a mean amount of 1.1×10^5 pg/ml (range, 3.1×10^4 to 2.8×10^5 pg/ml). AK602 and ddI were found to significantly suppress the serum p24 amounts as examined on day 16 with a mean amount of 5.6×10^3 pg/ml (range, 8.1×10^2 to 2.1×10^4 pg/ml; $P = 0.001$) and 7.1×10^2 pg/ml (range, 1.3×10^2 to 1.1×10^4 pg/ml; $P = 0.001$), respectively (Fig. 6D).

AK602 suppressed R5 HIV-1 viremia in hu-PBMC-NOG mice. As described above, the PBMC transplanted to NOG mice were intensely activated in the xenogeneic environment and had undergone ~ 4 cycles of proliferation by day 2; a majority of the cells had undergone ≥ 10 cycles of proliferation by day 4 (Fig. 3B). These data suggested that R5 HIV-1 might extensively replicate in the hu-PBMC-NOG mice immediately after R5 HIV-1 inoculation. When we collected blood samples on days 5, 9, and 16 following the inoculation and determined R5 HIV-1 RNA copy numbers in infected, saline-treated mice ($n = 7$), the geometric mean copy number was 8.6×10^3 /ml (range, 1.7×10^3 to 1.0×10^5) on day 5 and rapidly increased to 1.9×10^5 /ml (range, 2.2×10^4 to 3.0×10^6) on day 9; by day 16, the mean copy number had reached 7.7×10^5 /ml (range, 2.6×10^5 to 3.0×10^6 /ml). However, AK602 significantly suppressed viremia by ~ 1.1 log, as examined on day 5; the mean numbers of R5 HIV-1 RNA copies in AK602-administered mice were 1.6 and 1.8 logs lower than those in saline-treated mice examined on days 9 and 16, respectively (Fig. 7). Comparable viremia suppression was seen in the mice receiving ddI (Fig. 7). It was noted that although AK602 did not completely prevent the viremia from further increasing after day 5, there was a clear reduction in the viremia increase rates. The mean slopes (change in RNA copies per day over the range of data from 5 to 16 days) for the group receiving saline was 0.167 ± 0.042 , whereas those for the AK602 and ddI groups were 0.102 ± 0.041 and 0.091 ± 0.037 , respectively. Thus, the rates of increase in the AK602 ($P = 0.0057$) and ddI ($P = 0.0023$) mice were significantly lower than that for the mice given saline, indicating that both of the agents significantly inhibited R5 HIV-1 replication in this mouse model over the range of days evaluated. No apparent AK602- or ddI-associated adverse effects were seen throughout the study period.

DISCUSSION

In the present hu-PBMC-NOG mouse model, human CD4⁺/CD8⁺ cell ratios went down to 0.1 by 16 days after R5 HIV-1 inoculation, the amounts of proviral DNA and p24 gag antigen reached 10^5 to 10^6 copies/ 10^5 CD4⁺ cells and 10^5 pg/ml, respectively (Fig. 6), and no mice failed to be infected with R5 HIV-1. It is noteworthy that the use of NOG mice provides a higher engraftment rate than with other SCID mice such as NOD/Shi-SCID mice treated with anti-NK cell antibody or the β_2 -microglobulin-deficient NOD-SCID mice (10). With NOG mice, the chimeric rate of 30 to 40% is achieved, and cord blood CD34⁺ cells have been shown to "take" with as few as 100 cells (10). Moreover, all infected mice developed high levels of R5 HIV-1 viremia by day 16, reaching as high as 10^6 copies/ml (Fig. 7). It is worth noting that the notably high levels of HIV-1 viremia seen in the present mouse model by 16 days after R5 HIV-1 exposure can be seen only on acute infection or up to 10 years after HIV infection in humans (3, 4).

In the present study, we found that the conspicuous susceptibility to the infectivity and replication of R5 HIV-1 in these mice appeared to stem from the hyperactivation of the implanted human PBMC. The implanted PBMC were highly activated in the xenogeneic environment, expressed quite high

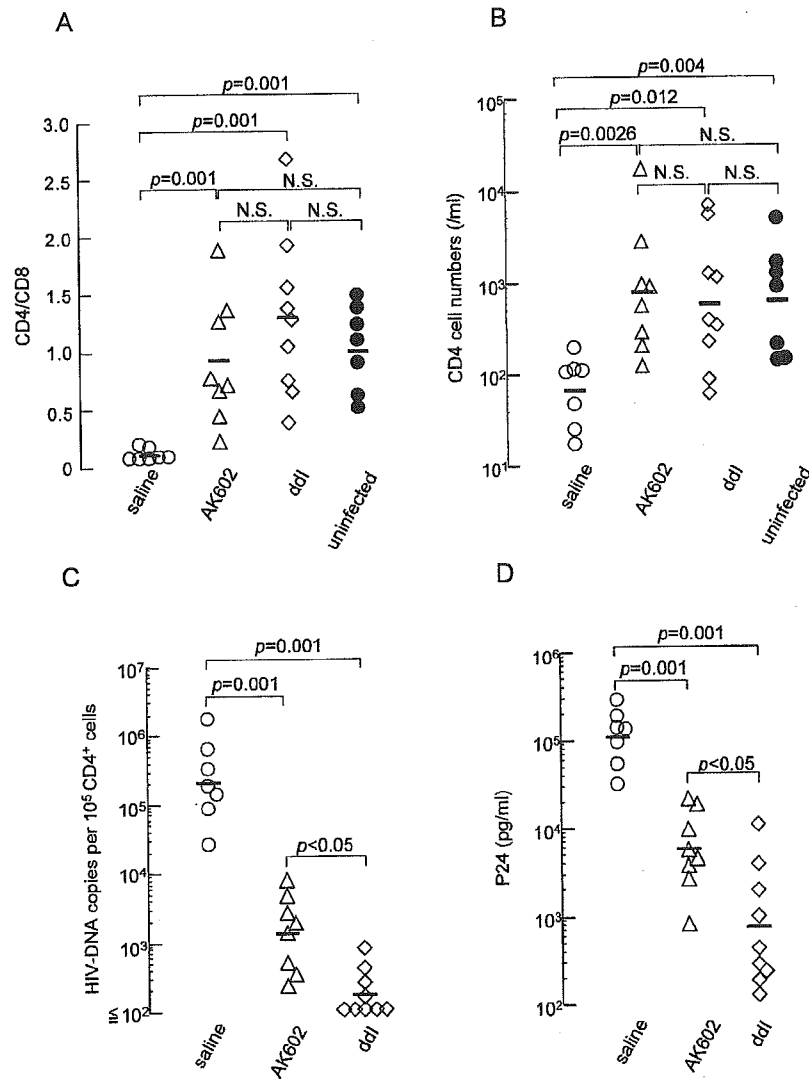


FIG. 6. Effects of AK602 on CD4⁺/CD8⁺ ratios and the amounts of proviral DNA and HIV-1 p24 in infected hu-PBMC-NOG mice. (A) Overall profiles of CD4⁺/CD8⁺ cell ratios. Note that the mean CD4⁺/CD8⁺ cell ratio in mice given saline (*n* = 7) was 0.1, while those in mice given AK602 or ddi were 0.92 and 1.29, respectively. The mean ratio in uninfected mice was 1.0. (B) Numbers of CD4⁺ cells per microliter in each mouse group. (C) HIV-1 proviral DNA copy numbers in CD4⁺ cells from each mouse group were determined by real-time PCR assay. Values are shown per 10⁵ CD4⁺ cells, as described in Materials and Methods. Note that the mean number of HIV-1 proviral DNA copies was 2.0 × 10⁵ per 10⁵ CD4⁺ cells in mice given saline, while those in AK602- and ddi-treated groups were 1.3 × 10³ and 1.8 × 10² per 10⁵ CD4⁺ cells (both, *P* = 0.001), respectively. (D) Amounts of plasma p24 antigen. Note that the amounts of p24 in plasma were high in saline-treated mice while AK602 and ddi significantly suppressed the serum p24 amounts as examined on day 16 after HIV-1_{Ba-L} inoculation. The short bars indicate the arithmetic (A) and geometric (B, C, and D) means obtained.

levels of HLA-DR, and rapidly and continuously proliferated immediately after intraperitoneal infusion (Fig. 3A, B, and D). Moreover, the implanted PBMC expressed as much as 2.8-fold-higher levels of CCR5 on day 3 following implantation compared to PHA-PBMC on day 3 in culture (Fig. 3E). The combination of rapid proliferation and high levels of CCR5 expression of the implanted PBMC should explain the reason R5 HIV-1 rapidly replicated in the hu-PBMC-NOG mice and presented such high levels of R5 HIV-1 viremia. In this regard, only a few groups to date have documented the levels of viremia in the scientific literature. Among them are those by Garaci et al. (8) and Koyanagi et al. (14). The former documented

high levels of viremia with a peak of 2.67 × 10⁶ copies/ml in hu-PBL-NOD-SCID mice in which HIV-1-infected macrophages were inoculated, unlike our NOG mouse model where HIV-1 was directly inoculated. The latter report by Koyanagi et al. does not have viremia data but has data on p24 levels with a geometric mean of 11,092 pg/ml on day 14 after HIV-1 inoculation. However, the variation was much greater (178 to 1,434,444 pg/ml). Thus, one can say that the present model provides a greater reproducibility of high viremia levels than the mouse system reported by Koyanagi (14). It should be noted that the high levels of viremia and high engraftment rate achieved in this mouse model made it possible to monitor the

TABLE 2. Comparison of HIV-1 proviral DNA in human CD4⁺ and CD4⁻ cell fractions^a

Sample	HIV-1 DNA copies (10 ⁵ cells)		
	SCID-PBMC	CD4 ⁺ cells	CD4 ⁻ cells
Saline 1	138,858	162,193	461
Saline 2	135,967	117,949	<100
Saline 3	83,863	94,590	<100
AK602 1	3,390	2,300	<100
AK602 2	5,575	4,606	<100
AK602 3	1,925	1,398	<100
ddI 1	301	516	<100
ddI 2	793	1,317	<100
ddI 3	<100	118	<100

^a HIV-1 proviral DNA copy numbers were determined by real-time PCR assay of unseparated human PBMC and purified CD4⁺ and CD4⁻ cells, following recovery from hu-PBMC-NOG mice. Values are shown per 10⁵ cells, as described in Materials and Methods.

changes in the viremia levels periodically in the same set of mice without sacrificing them, while most of the previously described SCID mouse models required mice to be sacrificed at each time point of testing (25, 29, 30) or needed further in vitro coculture of the PBMC recovered from the mice with freshly prepared uninfected target cells for an additional period of days (9, 34).

We demonstrated in this study that a novel SDP derivative, AK602, exerted highly potent activity against laboratory and primary R5 HIV-1 strains as well as MDR R5 HIV-1 variant with IC₅₀ values of subnanomolar concentrations (Table 1). It should be noted that AK602 represents a novel SDP derivative, which binds to human CCR5 but not to human CXCR4, CCR1, CCR2, CCR3, CCR4 or murine CCR5; blocks the binding of MIP-1 α to CCR5 with an extremely high affinity (K_d values of \sim 3 nM); potently blocks HIV-1-gp120/CCR5 binding; and exerts potent activity against a wide spectrum of laboratory and primary R5 HIV-1 isolates including MDR HIV-1 and HIV-1 strains of various clades with IC₅₀ values of 0.2 to 0.6 nM in vitro (K. Maeda, H. Ogata, S. Harada, Y. Tojo, T. Miyakawa, H. Nakata, Y. Takaoka, S. Shibayama, D. Fukushima, J. Moravek, E. Arnold, and H. Mitsuya, 11th Conf. Retrovir. Opp. Infect., abstr. 540, 2004; J. Demarest et al., XV Int. AIDS Conf., abstr. WeOrA1231, 2004). The plasma half-life of AK602 in the hu-PBMC-NOG mice, however, proved to be as short as 29 min when the agent was administered intraperitoneally (Fig. 4A). Considering that AK602 possesses such a high binding affinity to CCR5, we presumed that AK602 could remain on CCR5 for an extended period of time even after the agent was removed from the bloodstream in mice. The high and extensive level of AK602 occupancy observed in PBMC recovered from mice receiving AK602 substantiated this presumption (Fig. 4D). The subsequent in vitro experiment in which CCR5⁺ MAGI cells were incubated with AK602 but exposed to R5 HIV-1 after the removal of the compound from the culture medium showed that AK602's anti-R5 HIV-1 activity can persist for an extensive period of time even if AK602 is no longer present in the culture (Fig. 4E). It is of note that unlike certain reports of in vivo anti-HIV-1 activity of

chemokine antagonists which were administered before HIV-1 inoculation, thus demonstrating prophylactic effects of such agents (9, 30), the present system demonstrates anti-HIV-1 treatment after the establishment of HIV-1 infection, analogous to antiviral therapy in clinical settings.

When highly active antiretroviral therapy exerts its potent antiviral effects in clinical settings, a decrease in HIV-1 viremia is seen often within weeks, ultimately resulting in undetectable viremia; however in the present study, the viremia levels in mice receiving AK602 or ddI continued to increase although the rate of increment significantly declined (Fig. 7). The failure of AK602 and ddI to decrease viremia levels could be due in part to such a rapid viral replication in hyperactivated and proliferating CD4⁺ cells. As discussed earlier, PBMC recovered from the hu-PBMC-NOG mice were highly positive for CCR5 and HLA-DR (Fig. 3D and E), compared to the levels of activation seen in the same donor's PHA-PBMC. It should be noted, however, that the mean numbers of proviral DNA copies on day 16 in mice receiving AK602 and ddI were 1.3×10^3 and 1.8×10^2 per 10⁵ CD4⁺ cells, respectively (Fig. 6C), suggesting that most CD4⁺ cells (98.7 and 99.8% on average, respectively) were free of HIV-1 and proliferating in those

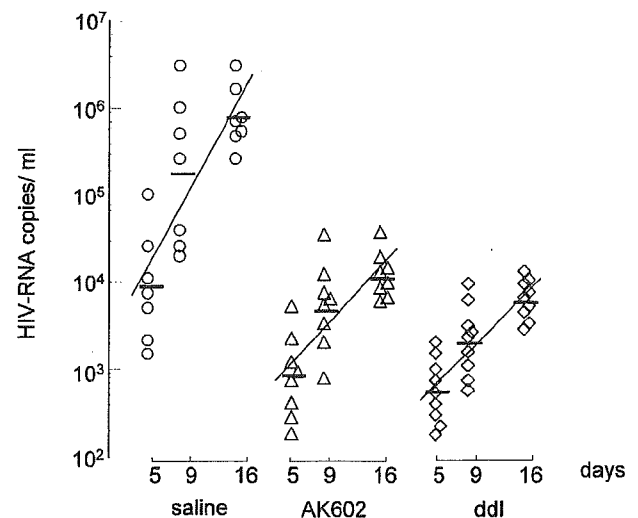


FIG. 7. AK602 suppresses R5 HIV-1 viremia in hu-PBMC-NOG mice. Blood samples were collected on days 5, 9, and 16 after inoculation and were subjected to the determination of R5 HIV-1 RNA copy numbers. Note that the copy numbers in saline-treated mice rapidly increased and reached $\sim 10^6$ /ml by day 16, while AK602 significantly suppressed the viremia by 1.6 and 1.8 logs as examined on day 9 ($P = 0.001$ compared to saline-treated mice) and day 16 ($P = 0.001$), respectively. Comparable viremia suppression was seen in ddI-treated mice, except on day 16, when ddI activity was greater than that of AK602 ($P = 0.027$). Note that there was a clear reduction in the rate of increase of viremia as well. When the values of log₁₀ HIV-1 RNA copies were calculated and the slopes corresponding to the rates of increase per day were determined, the resulting mean slope (solid line) for the saline-treated mice was 0.167 ± 0.042 , whereas those for the AK602- and ddI-treated mice were 0.102 ± 0.041 and 0.091 ± 0.037 , respectively. The increase rate for saline-treated mice was significantly higher than those of AK602-treated mice ($P = 0.0057$) and ddI-treated mice ($P = 0.0023$), respectively. The horizontal bars and solid lines represent the geometric means of HIV-1 RNA copy numbers and the slopes calculated, respectively.

mice on day 16 after the virus inoculation, if one copy of proviral DNA was postulated to reside in one CD4⁺ cell.

One of us (Y.K.) previously attempted to investigate the mechanism of CD4⁺ cell depletion seen in individuals with HIV-1 infection by employing a PBMC-transplanted NOD (NOD/Shi) *scid/scid* mouse system (24). Massive apoptosis was observed in HIV-1-uninfected CD4⁺ cells in the spleens of the HIV-1-infected NOD-*scid/scid* mice. A combination of terminal deoxynucleotidyl transferase-mediated dUTP nick-end labeling and immunostaining for death-inducing tumor necrosis factor (TNF) family molecules showed that apoptotic cells were frequently found in conjugation with TNF-related apoptosis-inducing ligand (TRAIL)-expressing CD3⁺ CD4⁺ human T cells. Further observation that a neutralizing anti-TRAIL antibody inhibited the development of CD4⁺ cell apoptosis suggested that a large number of HIV-1-uninfected CD4⁺ cells undergo TRAIL-mediated apoptosis, contributing to the marked depletion of CD4⁺ cells (24). The observation by Miura and his colleagues that the number of TRAIL-positive cells was consistently higher in HIV-1-infected mice than in uninfected ones makes it apparent that TRAIL expression is induced upon HIV-1 infection (23, 24). In this regard, the present observation that AK602 and ddI potently blocked the decrease in CD4⁺ cells in spite of the rather increasing HIV-1 viremia in the face of AK602 or ddI (Fig. 7) suggests that the mere presence of viremia might not be sufficient for the HIV-induced apoptosis in CD4⁺ cells. Our observation that most surviving CD4⁺ cells in mice receiving AK602 or ddI were free of HIV-1 (see above) suggests that these anti-HIV-1 agents might block not only de novo HIV-1 infection, but also bystander killing of uninfected CD4⁺ cells. The present data also suggest that a certain factor(s) such as cytokines produced by the freshly HIV-1-infected cells might mediate the apoptosis of bystander CD4⁺ cells through the upregulation of TRAIL expression, death receptors (e.g., DR4 and DR5), and/or downregulation of decoy receptors (e.g., DcR1 and DcR2) (26, 27). However, experiments with a combination of terminal deoxynucleotidyl transferase-mediated dUTP nick-end labeling and TNF family molecules have to be conducted for better understanding of the bystander killing in regard to AK602's effects.

It is of note that several CCR5 antagonists are currently in various stages of development. AK602 has recently been administered to healthy adult subjects in a phase I clinical trial and shown to bind to CCR5 for an extended period of time, suggesting that an oral formulation with fewer administrations and lower dosage is possible for AK602 as a therapeutic agent for HIV-1 infection (J. Demarest, K. Adkison, S. Sparks, A. Shachoy-Clark, K. Schell, S. Reddy, L. Fang, K. O'Mara, S. Shibayama, and S. Piscitelli, 11th Conf. Retrovir. Opp. Infect., abstr. 139, 2004). Taken together, our observations that plasma viral load reached ~10⁶ RNA copies/ml and that AK602 potently inhibited the replication of R5 HIV-1 strongly suggest that the present hu-PBMC-NOG mouse AIDS model could serve as a useful instrument for analyzing the pathogenesis of HIV-1 infection and testing the efficacy of antiviral agents.

ACKNOWLEDGMENTS

We thank Seth Steinberg for statistical analysis and Naoko Misawa, Yuji Kawano, and Hiroshi Ogata for technical assistance and discussion.

This work was supported in part by grant-in-aids for Scientific Research on Priority Areas (14207025 and 15019086) from the Japanese Ministry of Education, Science, Sports, Culture and Technology of Japan (Monbu-Kagakusho) and a grant for AIDS Research (H15-AIDS-001) from the Ministry of Health, Labor, and Welfare of Japan (Kosei-Rohdoshu).

REFERENCES

- Baba, M., O. Nishimura, N. Kanzaki, M. Okamoto, H. Sawada, Y. Iizawa, M. Shiraishi, Y. Aramaki, K. Okonogi, Y. Ogawa, K. Meguro, and M. Fujino. 1999. A small-molecule, nonpeptide CCR5 antagonist with highly potent and selective anti HIV-1 activity. *Proc. Natl. Acad. Sci. USA* 96:5698-5703.
- Carr, A., K. Samaras, A. Thorisdottir, G. R. Kaufmann, D. J. Chisholm, and D. A. Cooper. 1999. Diagnosis, prediction, and natural course of HIV-1 protease-inhibitor associated lipodystrophy, hyperlipidaemia, and diabetes mellitus: a cohort study. *Lancet* 353:2093-2099.
- Dean, M., M. Carrington, C. Winkler, G. A. Huttley, M. W. Smith, R. Allikmets, J. J. Goedert, S. P. Buchbinder, E. Vittinghoff, E. Gomperts, S. Donfield, D. Vlahov, R. Kaslow, A. Saah, C. Rinaldo, R. Detels, and S. J. O'Brien. 1996. Genetic restriction of HIV-1 infection and progression to AIDS by a deletion allele of the CCR5 structural gene. Hemophilia Growth and Development Study, Multicenter AIDS Cohort Study, Multicenter Hemophilia Cohort Study, San Francisco City Cohort, ALIVE Study. *Science* 273:1856-1862.
- Easterbrook, P. J. 1999. Long-term non-progression in HIV infection: definitions and epidemiological issues. *J. Infect.* 38:71-73.
- Fauci, A. S. 1999. The AIDS epidemic—considerations for the 21st century. *N. Engl. J. Med.* 341:1046-1050.
- Finzi, D., J. Blankson, J. D. Siliciano, J. B. Margolick, K. Chadwick, T. Pierson, K. Smith, J. Lisiewicz, F. Lori, C. Flexner, T. C. Quinn, R. E. Chaisson, E. Rosenberg, B. Walker, S. Gange, J. Gallant, and R. F. Siliciano. 1999. Latent infection of CD4⁺ T cells provides a mechanism for lifelong persistence of HIV-1, even in patients on effective combination therapy. *Nat. Med.* 5:512-517.
- Gartner, S., P. Markovits, D. M. Markovitz, M. H. Kaplan, R. C. Gallo, and M. Popovic. 1986. The role of mononuclear phagocytes in HTLV-III/LAV infection. *Science* 233:215-219.
- Garaci, E., S. Aquaro, C. Lapenta, A. Amendola, M. Spada, S. Covaceuszach, C. F. Perno, and F. Belardelli. 2003. Anti-nerve growth factor Ab abrogates macrophage-mediated HIV-1 infection and depletion of CD4⁺ T lymphocytes in hu-SCID mice. *Proc. Natl. Acad. Sci. USA* 100:8927-8932.
- Ichiyama, K., S. Yokoyama-Kumakura, Y. Tanaka, R. Tanaka, K. Hirose, K. Bannai, T. Edamatsu, M. Yanaka, Y. Niitani, N. Miyano-Kurosaki, H. Takaku, Y. Koyanagi, and N. Yamamoto. 2003. A duodenally absorbable CXC chemokine receptor 4 antagonist, KRH-1636, exhibits a potent and selective anti-HIV-1 activity. *Proc. Natl. Acad. Sci. USA* 100:4185-4190.
- Ito, M., H. Hiramatsu, K. Kobayashi, K. Suzue, M. Kawabata, K. Hioki, Y. Ueyama, Y. Koyanagi, K. Sugamura, K. Tsuji, T. Heike, and T. Nakahata. 2002. NOD/SCID γ (c)(null) mouse: an excellent recipient mouse model for engraftment of human cells. *Blood* 100:3175-3182.
- Kavlick, M. F., and H. Mitsuya. 2001. The emergence of drug resistant HIV-1 variants and its impact on antiretroviral therapy of HIV-1 infection, p. 279-312. *In* E. De Clercq (ed.), *The art of antiretroviral therapy*. American Society for Microbiology, Washington, D.C.
- Koh, Y., H. Nakata, K. Maeda, H. Ogata, G. Bilcer, T. Devasamudram, J. F. Kincaid, P. Boross, Y. F. Wang, Y. Tie, P. Volarath, L. Gaddis, R. W. Harrison, I. T. Weber, A. K. Ghosh, and H. Mitsuya. 2003. Novel bis-tetrahydrofuranylurethane-containing nonpeptidic protease inhibitor (PI) UIC-94017 (TMC114) with potent activity against multi-PI-resistant human immunodeficiency virus in vitro. *Antimicrob. Agents Chemother.* 47:3123-3129.
- Koyanagi, Y., S. Miles, R. T. Mitsuyasu, J. E. Merrill, H. V. Vinters, and I. S. Chen. 1987. Dual infection of the central nervous system by AIDS viruses with distinct cellular tropisms. *Science* 236:819-822.
- Koyanagi, Y., Y. Tanaka, J. Kira, M. Ito, K. Hioki, N. Misawa, Y. Kawano, K. Yamasaki, R. Tanaka, Y. Suzuki, Y. Ueyama, E. Terada, T. Tanaka, M. Miyasaka, T. Kobayashi, Y. Kumazawa, and N. Yamamoto. 1997. Primary human immunodeficiency virus type 1 viremia and central nervous system invasion in a novel hu-PBL-immunodeficient mouse strain. *J. Virol.* 71:2417-2424.
- Lee, B., M. Sharron, L. J. Montaner, D. Weissman, and R. W. Doms. 1999. Quantification of CD4, CCR5, and CXCR4 levels on lymphocyte subsets, dendritic cells, and differentially conditioned monocyte-derived macrophages. *Proc. Natl. Acad. Sci. USA* 96:5215-5220.
- Lyons, A. B. 2000. Analysing cell division in vivo and in vitro using flow cytometric measurement of CFSE dye dilution. *J. Immunol. Methods* 243: 147-154.
- Maeda, K., K. Yoshimura, S. Shibayama, H. Habashita, H. Tada, K. Sagawa, T. Miyakawa, M. Aoki, D. Fukushima, and H. Mitsuya. 2001. Novel low molecular weight spirodiketopiperazine derivatives potently inhibit R5

- HIV-1 infection through their antagonistic effects on CCR5. *J. Biol. Chem.* 276:35194-35200.
18. Maeda, Y., M. Foda, S. Matsushita, and S. Harada. 2000. Involvement of both the V2 and V3 regions of the CCR5-tropic human immunodeficiency virus type 1 envelope in reduced sensitivity to macrophage inflammatory protein 1 α . *J. Virol.* 74:1787-1793.
 19. McCune, J. M., R. Namikawa, C. C. Shih, L. Rabin, and H. Kaneshima. 1990. Suppression of HIV infection in AZT-treated SCID-hu mice. *Science* 247:564-566.
 20. Mitsuya, H., and S. Broder. 1986. Inhibition of the in vitro infectivity and cytopathic effect of human T-lymphotropic virus type III/lymphadenopathy virus-associated virus (HTLV-III/LAV) by 2',3'-dideoxynucleosides. *Proc. Natl. Acad. Sci. USA* 83:1911-1915.
 21. Mitsuya, H., and S. Broder. 1987. Strategies for antiviral therapy in AIDS. *Nature* 325:773-778.
 22. Mitsuya, H., and J. Erickson. 1999. Discovery and development of antiretroviral therapeutics for HIV infection, p. 751-780. *In* T. C. Merigan, J. G. Bartlet, and D. Bolognesi (ed.), *Textbook of AIDS medicine*. Williams & Wilkins, Baltimore, Md.
 23. Miura, Y., N. Misawa, Y. Kawano, H. Okada, Y. Inagaki, N. Yamamoto, M. Ito, H. Yagita, K. Okumura, H. Mizusawa, and Y. Koyanagi. 2003. Tumor necrosis factor-related apoptosis-inducing ligand induces neuronal death in a murine model of HIV central nervous system infection. *Proc. Natl. Acad. Sci. USA* 100:2777-2782.
 24. Miura, Y., N. Misawa, N. Maeda, Y. Inagaki, Y. Tanaka, M. Ito, N. Koyanagi, N. Yamamoto, H. Yagita, H. Mizusawa, and Y. Koyanagi. 2001. Critical contribution of tumor necrosis factor-related apoptosis-inducing ligand (TRAIL) to apoptosis of human CD4+ T cells in HIV-1-infected hu-PBL-NOD-SCID mice. *J. Exp. Med.* 193:651-660.
 25. Mosier, D. E., R. J. Gulizia, S. M. Baird, D. B. Wilson, D. H. Spector, and S. A. Spector. 1991. Human immunodeficiency virus infection of human-PBL-SCID mice. *Science* 251:791-794.
 26. Pan, G., J. Ni, Y. F. Wei, G. Yu, R. Gentz, and V. M. Dixit. 1997. An antagonist decoy receptor and a death domain-containing receptor for TRAIL. *Science* 277:815-818.
 27. Pan, G., K. O'Rourke, A. M. Chinnaiyan, R. Gentz, R. Ebner, J. Ni, and V. M. Dixit. 1997. The receptor for the cytotoxic ligand TRAIL. *Science* 276:111-113.
 28. Ratain, M., and W. Plunkett. 1997. Pharmacology, p. 875-889. *In* J. Holland, R. Bast, Jr., D. Morton, E. Frei, D. KuFe, and R. Weichselbaum (ed.), *Cancer medicine*, 4th ed. Williams and Wilkins, Baltimore, Md.
 29. Ruxrungtham, K., E. Boone, H. Ford, Jr., J. S. Driscoll, R. T. Davey, Jr., and H. C. Lane. 1996. Potent activity of 2'- β -fluoro-2',3'-dideoxyadenosine against human immunodeficiency virus type 1 infection in hu-PBL-SCID mice. *Antimicrob. Agents Chemother.* 40:2369-2374.
 30. Strizki, J. M., S. Xu, N. E. Wagner, L. Wojcik, J. Liu, Y. Hou, M. Endres, A. Palani, S. Shapiro, J. W. Clader, W. J. Greenlee, J. R. Tagat, S. McCombie, K. Cox, A. B. Fawzi, C. C. Chou, C. Pugliese-Sivo, L. Davies, M. E. Moreno, D. D. Ho, A. Trkola, C. A. Stoddart, J. P. Moore, G. R. Reyes, and B. M. Baroudy. 2001. SCH-C (SCH 351125), an orally bioavailable, small molecule antagonist of the chemokine receptor CCR5, is a potent inhibitor of HIV-1 infection in vitro and in vivo. *Proc. Natl. Acad. Sci. USA* 98:12718-12723.
 31. Walker, U. A., B. Setzer, and N. Venhoff. 2002. Increased long-term mitochondrial toxicity in combinations of nucleoside analogue reverse-transcriptase inhibitors. *AIDS* 16:2165-2173.
 32. Westervelt, P., H. E. Gendelman, and L. Ratner. 1991. Identification of a determinant within the human immunodeficiency virus 1 surface envelope glycoprotein critical for productive infection of primary monocytes. *Proc. Natl. Acad. Sci. USA* 88:3097-3101.
 33. Yahata, T., K. Ando, Y. Nakamura, Y. Ueyama, K. Shimamura, N. Tamaoki, S. Kato, and T. Hotta. 2002. Functional human T lymphocyte development from cord blood CD34+ cells in nonobese diabetic/Shi-scid, IL-2 receptor gamma null mice. *J. Immunol.* 169:204-209.
 34. Yoshida, A., R. Tanaka, T. Murakami, Y. Takahashi, Y. Koyanagi, M. Nakamura, M. Ito, N. Yamamoto, and Y. Tanaka. 2003. Induction of protective immune responses against R5 human immunodeficiency virus type 1 (HIV-1) infection in hu-PBL-SCID mice by intrasplenic immunization with HIV-1-pulsed dendritic cells: possible involvement of a novel factor of human CD4(+) T-cell origin. *J. Virol.* 77:8719-8728.
 35. Yoshimura, K., R. Kato, K. Yusa, M. F. Kavlick, V. Maroun, A. Nguyen, T. Mimoto, T. Ueno, M. Shintani, J. Falloon, H. Masur, H. Hayashi, J. Erickson, and H. Mitsuya. 1999. JE-2147: a dipeptide protease inhibitor (PI) that potently inhibits multi-PI-resistant HIV-1. *Proc. Natl. Acad. Sci. USA* 96:8675-8680.

Structure-Based Design: Synthesis and Biological Evaluation of a Series of Novel Cycloamide-Derived HIV-1 Protease Inhibitors

Arun K. Ghosh,^{*,†} Lisa M. Swanson,[†] Hanna Cho,[†] Sofiya Leshchenko,[†] Khaja Azhar Hussain,[†] Stephanie Kay,[†] D. Eric Walters,[‡] Yasuhiro Koh,[§] and Hiroaki Mitsuya^{§,||}

Department of Chemistry, University of Illinois at Chicago, 845 West Taylor Street, Chicago, Illinois 60607, Department of Biological Chemistry, Rosalind Franklin University of Medicine and Science, North Chicago, Illinois 60064, Department of Hematology and Infectious Diseases, Kumamoto University School of Medicine, Kumamoto 860-8556, Japan, and Experimental Retrovirology Section, HIV and AIDS Malignancy Branch, National Cancer Institute, Bethesda, Maryland 20892

Received January 8, 2005

The structure-based design and synthesis of a series of novel nonpeptide HIV protease inhibitors are described. The inhibitors were designed based upon the X-ray crystal structure of inhibitor **1** (UIC-94017)-bound HIV-1 protease. The inhibitors incorporated 3-hydroxysalicylic acid-derived acyclic and cyclic P₂ ligand into the (*R*)-(hydroxyethylamino)sulfonamide isostere. The inhibitors contain only two chiral centers and are readily synthesized in optically active form utilizing Sharpless asymmetric epoxidation, regioselective epoxide opening, and ring-closing olefin metathesis using Grubbs' catalyst as the key steps. We have synthesized 13–15-membered cycloamides and evaluated their HIV-1 protease enzyme inhibitory and antiviral activities in MT-2 cells. Interestingly, all cycloamide-derived inhibitors are noticeably more potent than the corresponding acyclic compounds. The ring size and substituent effects were investigated. It turned out that the 14-membered saturated ring is preferred by the S₁–S₂ active sites of HIV-1 protease. Macrocycle **26** showed excellent enzyme inhibitory potency with a K_i value of 0.7 nM and an antiviral IC₅₀ value of 0.3 μM. In view of their structural simplicity and preliminary interesting results, further optimization of these inhibitors is underway.

Introduction

The global pandemic of HIV/AIDS is one of the most extraordinary humanitarian and medical challenges of our time. Combination therapy or highly active anti-retroviral therapy with HIV protease inhibitors and reverse transcriptase inhibitors has become the major current treatment regimen for AIDS.¹ Our recent structure-based designed strategies enhancing backbone binding led to the discovery of a nonpeptidyl HIV protease inhibitor **1** (UIC-94017, now renamed as TMC-114; Figure 1), which is exceedingly potent against wild-type (K_i = 15 ± 1 pM, n = 4 and ID₅₀ = 1.4 ± 0.25 nM, n = 5) and resistant viruses.^{2,3} It is currently undergoing advanced clinical trials.⁴ In inhibitor **1**, we incorporated a structure-based designed bis-tetrahydrofuran as the P₂ ligand in (*R*)-(hydroxyethylamino)sulfonamide isostere.⁵ A high-resolution X-ray crystal structure of this inhibitor-bound HIV-1 protease structure revealed critical ligand-binding site interaction in the HIV protease active site.⁶ Upon the basis of this structure, we subsequently speculated that various 13–15-membered macrocycles involving P₁–P₂ ligands would effectively hydrogen bond with the critical Asp-29 and Asp-30 backbone residues and tight-bound water molecule as well as fill in the hydrophobic pockets of S₁–S₂ binding sites. In an effort to introduce structural diversity, we have designed and explored 2,3-dihydroxybenzoic acid-

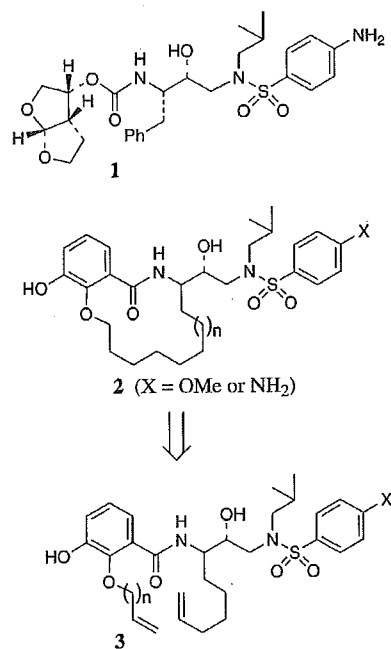


Figure 1. Structures of inhibitors **1** and cyclic and acyclic inhibitors.

derived 13–15-membered cycloamides as P₁–P₂ ligands, which could conceivably make critical interactions in the S₁–S₂ binding sites. Herein, we report our preliminary results of these investigations. The inhibitors were synthesized stereoselectively by using Sharpless asymmetric epoxidation and subsequent regioselective opening of epoxide rings as the key steps. Cycloamide

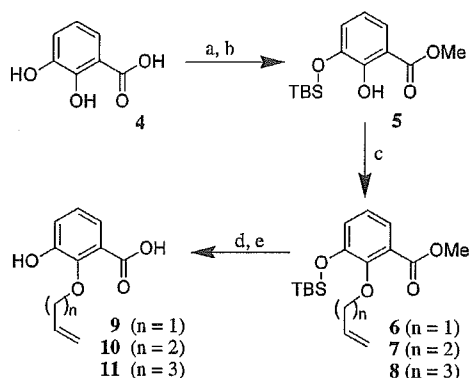
* To whom correspondence should be addressed. Tel: 312-996-9672. Fax: 312-996-1547. E-mail: arunghos@uic.edu.

[†] University of Illinois at Chicago.

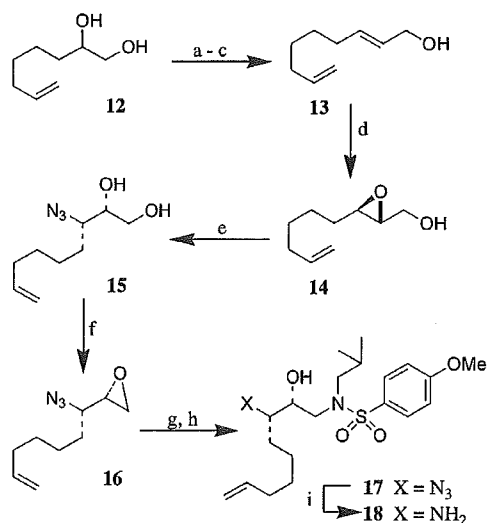
[‡] Rosalind Franklin University of Medicine and Science.

[§] Kumamoto University School of Medicine.

^{||} National Cancer Institute.

Scheme 1^a

^a Reagents and conditions: (a) Cs_2CO_3 , $\text{MeOH-H}_2\text{O}$, 23 °C; then MeI , DMF , 0–23 °C. (b) TBSCl , $i\text{-Pr}_2\text{NEt}$, DMF , 0 °C. (c) Allylic alcohol, DEAD , PPh_3 , THF , 23 °C. (d) TBAF , THF , 0 °C. (e) LiOH , THF , H_2O , 55 °C.

Scheme 2^a

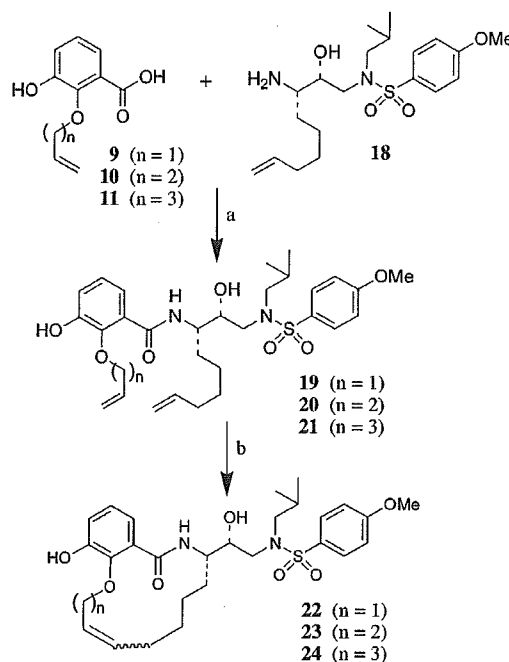
^a Reagents and conditions: (a) NaIO_4 , THF , H_2O , 23 °C. (b) $(\text{EtO})_2\text{POCH}_2\text{CO}_2\text{Et}$, NaH , THF , 0–23 °C. (c) DIBAL-H , CH_2Cl_2 , –78 °C. (d) $(-)\text{-DET}$, 4 Å MS , $\text{Ti}(i\text{-OPr})_4$, TBHP , CH_2Cl_2 , –20 °C. (e) $\text{Ti}(i\text{-OPr})_4$, TMSN_3 , benzene, 90 °C. (f) $\text{AcOCMe}_2\text{COCl}$, CHCl_3 , 0 °C; then NaOMe , THF , 23 °C. (g) $(\text{CH}_3)_2\text{CHCH}_2\text{NH}_2$, $i\text{-PrOH}$, 90 °C. (h) 4-MeO-Ph- SO_2Cl , 1:1 (CH_2Cl_2 , aqueous NaHCO_3), 23 °C. (i) LiAlH_4 , THF , 23 °C.

58 derivatives were prepared efficiently by using ring-
59 closing olefin metathesis.

Chemistry

61 The synthesis of 3-hydroxysalicylic acid-based non-
62 peptidyl P_2 ligands is illustrated in Scheme 1. Esteri-
63 fication of commercially available 3-hydroxysalicylic
64 acid with Cs_2CO_3 in MeOH followed by selective protec-
65 tion of the 3-hydroxyl group as the TBS ether provided
66 **5** in 78% yield. Ester **5** was then converted to allyl ethers
67 and its homologues (**6–8**) using Mitsunobu conditions⁷
68 in 58–89% yields. Removal of the TBS ether followed
69 by saponification of the ester afforded various acids
70 **9–11** in 83–94% yields.

71 Enantioselective synthesis of requisite hydroxyethyl-
72 amine sulfonamide isostere is outlined in Scheme 2.
73 Commercially available diol **12** was converted to allylic
74 alcohol **13** in a three-step sequence involving (i) oxida-

Scheme 3^a

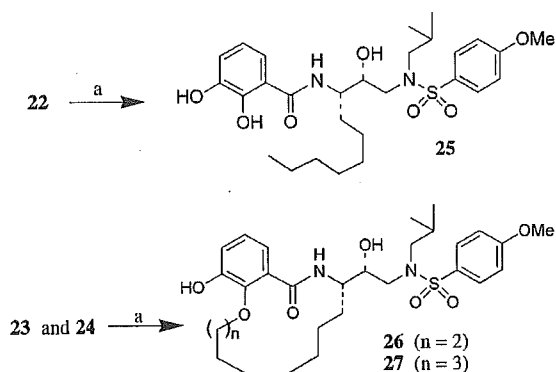
^a Reagents and conditions: (a) EDC , HOBT , Et_3N , DMF , 0–23 °C. (b) Grubbs' cat. (first generation), CH_2Cl_2 , 23 °C.

75 tive cleavage of diol **12** with NaIO_4 ; (ii) Horner-
76 Emmons olefination of the resulting aldehyde to α,β -
77 unsaturated ester; and (iii) DIBAL-H reduction of ester
78 to alcohol **13**. The allylic alcohol **13** was subjected to
79 the Sharpless asymmetric epoxidation⁸ condition with
80 $(-)$ -diethyl-D-tartrate to furnish the epoxide **14** in 78%
81 yield. Regioselective ring opening of epoxide **14** with
82 diisopropoxytitanium diazide in benzene at 90 °C, as
83 described by Sharpless and co-workers,⁹ provided the
84 azidiodiol **15** in near quantitative yield. The diol was
85 converted to the azidoepoxide **16** by treatment with
86 2-acetoxyisobutyryl chloride in chloroform at 23 °C
87 followed by exposure of the resulting chloroacetate
88 derivative to NaOMe to afford **16**.¹⁰ Sulfonamide **17**
89 was synthesized in a two-step sequence by first opening the
90 epoxide with isobutylamine and subsequent reaction of
91 the amine with *para*-methoxybenzenesulfonyl chloride
92 to afford sulfonamide **17** in 58% yield. Reduction of the
93 azides by LiAlH_4 furnished the amine **18**, which was
94 used directly for the next reaction without further
95 purification.

96 Synthesis of various acyclic inhibitors and subsequent
97 preparation of cyclic derivatives is carried out according
98 to Scheme 3. Using a standard peptide coupling proce-
99 dure,¹¹ amine **18** was reacted with carboxylic acids **9–11**
100 in the presence of *N*-ethyl-*N'*-(dimethylaminopropyl)-
101 carbodiimide hydrochloride (EDC), triethylamine, and
102 1-hydroxybenzotriazole hydrate (HOBT) in DMF to
103 furnish various acyclic inhibitors **19–21** in 50–76%
104 yields. Ring-closing olefin metathesis of these acyclic
105 derivatives with commercial first generation Grubbs'
106 catalyst¹² (10 mol %) in CH_2Cl_2 (0.003 M solution)
107 afforded 13–15-membered unsaturated cycloamides
108 **22–24** in excellent yield (89–96%).

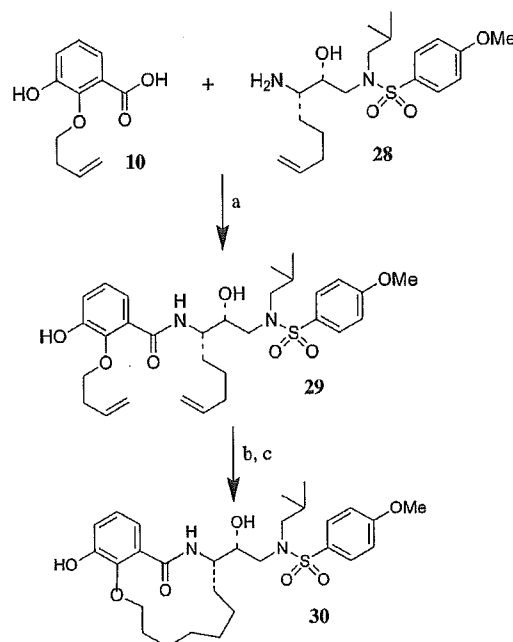
109 As shown in Scheme 4, catalytic hydrogenation of 13-
110 membered unsaturated inhibitor **22** in the presence

Scheme 4^a



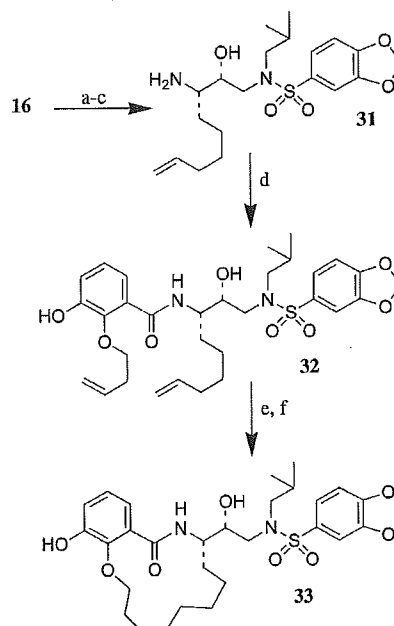
^a Reagents and conditions: (a) H₂, 10% Pd-C, MeOH, 23 °C.

Scheme 5^a



^a Reagents and conditions: (a) EDC, HOBT, Et₃N, DMF, 0–23 °C. (b) Grubbs' cat. (first generation), CH₂Cl₂, 23 °C. (c) H₂, 10% Pd-C, MeOH, 23 °C.

Scheme 6^a



^a Reagents and conditions: (a) (CH₃)₂CHCH₂NH₂, iPrOH, 90 °C. (b) 3,4-Methylenedioxybenzene sulfonyl chloride, CH₂Cl₂, aqueous NaHCO₃, 23 °C. (c) LiAlH₄, THF, 23 °C. (d) Acid 10, EDC, HOBT, Et₃N, DMF, 23 °C. (e) Grubbs' cat. CH₂Cl₂, 23 °C. (f) H₂, 10% Pd-C, MeOH, 23 °C.

of 10% Pd-C did not provide the corresponding saturated cycloamides. Instead, hydrogenation resulted in cleavage of the phenolic ether to give phenol **25** in 63% yield. Bergmann and Heimhold¹³ have previously reported similar cleavage of allylic ethers of phenol during hydrogenation reaction. Attempts to reduce the allylic double bond of **22** under different hydrogenation conditions (Lindlar catalyst, 5% Pd on BaSO₄, Rh on alumina, and Wilkinson's catalyst) failed to give the desired product, resulting in either the cleaved ether or the recovery of starting material. Besides hydrogenation, reduction with NaBH₄ and CoCl₂¹⁴ also resulted in the ether cleavage. Catalytic hydrogenation of the unsaturated cycloamides **23** and **24**, however, furnished the saturated macrocycles **26** and **27** in good yields (69–78%).

The synthesis of saturated 13-membered cycloamide was then carried out by an alternative route. Amino alcohol **28** was prepared enantioselectively following the route outlined in Scheme 2 from 5-hexenal, which was obtained by PCC oxidation of commercial 5-hexene-1-ol. Coupling of carboxylic acid **10** and amine **28** in the presence of EDC, HOBT, and Et₃N in DMF afforded the amide derivative **29**. It was converted to saturated 13-membered cycloamide derivative **30** in a two-step sequence by exposure of **29** to commercial first generation Grubbs' catalyst¹² (10 mol %) in CH₂Cl₂ followed by catalytic hydrogenation of the resulting unsaturated cycloamide in the presence of 10% Pd-C in methanol to provide **30** in 71% yield for two steps.

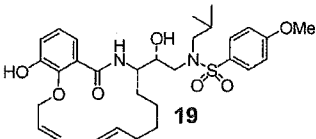
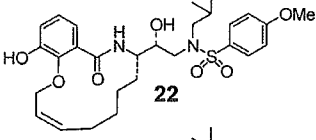
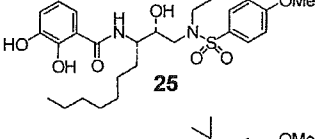
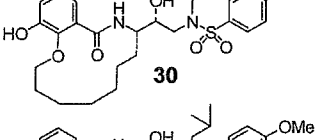
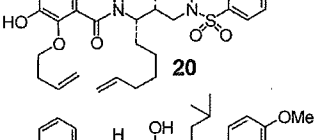
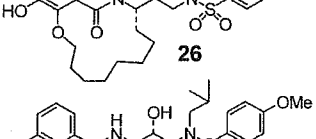
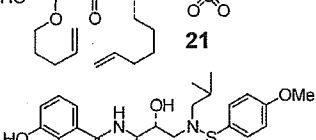
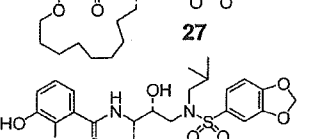
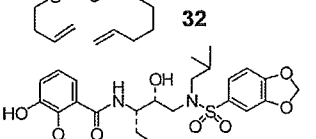
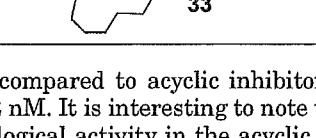
The synthesis of 14-membered inhibitor **33** was carried out as described in Scheme 6. Opening of epoxide **16** with isobutylamine and reaction of the resulting amine with 3,4-methylenedioxybenzene sulfonyl chloride¹⁵ followed by LAH reduction of the azide afforded the amine **31** in 61% yield. It was coupled with acid **10** under standard reaction conditions to furnish the acyclic inhibitor **32** in 57% yield. Exposure of **32** to Grubbs' catalyst¹² under dilute conditions (0.002 M CH₂Cl₂) afforded the corresponding unsaturated macrocycle, which upon hydrogenation furnished the saturated inhibitor **33** in 82% yield for two steps.

Biological Evaluation and Discussion

The inhibitory potencies of various acyclic and cyclic inhibitors in Table 1 were measured by the assay protocol of Toth and Marshall.¹⁷ The values with standard deviation denote the mean values from three

determinations. As can be seen, various saturated cycloamide-derived inhibitors have shown very impressive HIV-1 protease inhibitory activities. In general, the acyclic inhibitors were much less active than the corresponding macrocycles. Both 13-membered unsaturated inhibitor **22** and saturated inhibitor **30** with respective K_i values of 2 and 1 nM are significantly more

Table 1. Structure and Inhibitory Potencies of Various Acyclic and Cyclic Inhibitors

Entry No.	Compd	K_i (nM)
1.		12
2.		2 ± 0.15
3.		270
4.		1 ± 0.16
5.		2 ± 0.13
6.		0.7 ± 0.1
7.		9 ± 1.2
8.		2 ± 0.28
9.		20
10.		3 ± 0.33

165 potent as compared to acyclic inhibitor **19** with a K_i
 166 value of 12 nM. It is interesting to note the substantial
 167 loss in biological activity in the acyclic inhibitor **25** (K_i
 168 value of 270 nM) that resulted after cleavage of allylic
 169 ether. The 14-membered saturated macrocycle **26** with
 170 the *para*-methoxybenzenesulfonamide as the P_1' ligand
 171 is the most potent inhibitor in this series with a K_i value
 172 of 0.7 nM. The corresponding monounsaturated (inseparable
 173 5:1 *cis-trans* olefins) compound mixture displayed

Table 2. Antiviral Activity of Selected Compounds against HIV-1_{LAI}

inhibitor	IC ₅₀ (μ M)	IC ₇₅ (μ M)
20	>1	>1
26	0.30 ± 0.11	0.74 ± 0.15
27	0.56 ± 0.33	>1
33	>1	>1
saquinavir	0.012 ± 0.006	0.047 ± 0.011
amprenavir	0.028 ± 0.009	0.079 ± 0.011

a K_i value of 1 nM. The 15-membered inhibitor **27** has
 shown nearly a 3-fold attenuation in potency as compared
 to the 14-membered saturated cycloamide **26**. Because the
 14-membered saturated cycloamide **26** was the most potent,
 we have investigated the substituent effects on the P_1' aromatic
 sulfonamide ring. In this context, we incorporated a 1,3-*benzo*-
 dioxolane sulfonamide for the *para*-methoxybenzenesulfonamide.
 The inhibitory potency of the resulting saturated inhibitor **33**
 did not improve. The K_i value of the corresponding unsaturated
 macrocycle (inseparable 9:1 *cis-trans* olefins) was 4 nM,
 and the acyclic inhibitor **32** was significantly less potent.

We determined the antiviral activity of selected inhibitors.
 The results are summarized in Table 2. The IC₅₀ and IC₇₅ values
 shown were determined based on the inhibition of HIV-induced
 cytopathogenicity in MT-2 cells. All assays were conducted in
 duplicate, and the values with standard deviations denote the
 mean values from two or three. As can be seen, acyclic inhibitor
20 showed no antiviral activity. Inhibitors **26** and **27** (15-
 membered cycloamide) showed a moderate activity with antiviral
 IC₅₀ values of about 0.3 and 0.55 μ M, respectively. The
 antiviral activity of these compounds was substantially limited
 as compared to saquinavir¹⁸ or amprenavir.¹⁹ To improve
 antiviral potency, further modifications including incorporation
 of basic amine functionalities are in progress.

To gain insight into specific ligand-binding site interactions,
 an energy-minimized model structure of **26** was created
 (Figure 2). The structure was modeled in the active site of
 HIV-1 protease using the Molecular Operating Environment
 program (Chemical Computing Group, Montreal). The structure
 was built into the active site, based upon our published crystal
 structure of **1** complexed with HIV-1 protease (Protein Data
 Bank entry 1S6G) as a template.⁶ The conformation and
 placement of the inhibitor was manually adjusted, and then,
 minimization was carried out using the force field²⁰ with the
 protease structure fixed. Finally, minimization was carried
 out with all atom positions relaxed.

Upon the basis of this model, it appears that the 3-hydroxyl
 group of P2-salicylic acid derivative is within an effective
 hydrogen-bonding distance to Asp-29 (3.3 Å) in the S₂ region
 of the active site. Also, the P2-carbonyl can effectively
 hydrogen bond to the tight-bound water molecule. The
 flexible macrocyclic carbon chain fills the S1-S2 hydrophobic
 pockets. Furthermore, the key hydrogen-bonding interaction
 of the P_{2'}-OMe group and the Asp-29' is also quite apparent
 (distance 3.3 Å) as shown in Figure 2. However, the proper
 understanding of these active site interactions should await
 the solution of the X-ray crystal structure of a protein-ligand
 complex of **26**.²¹

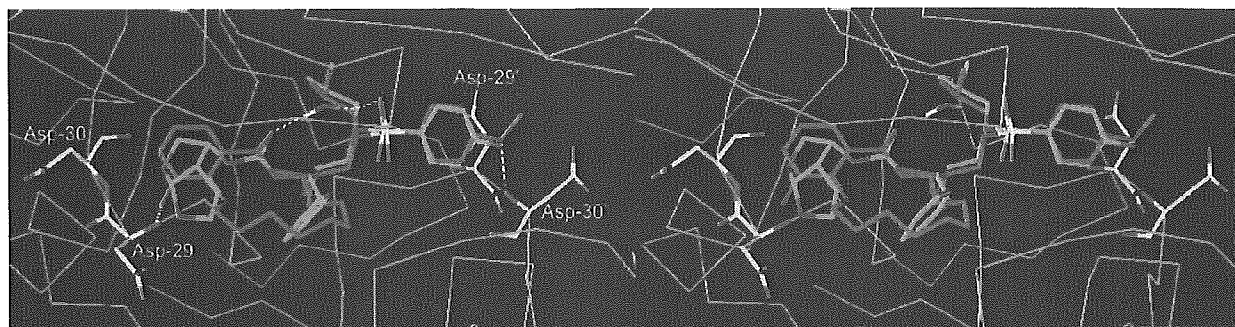


Figure 2. Stereoview of an energy minimized model structure of inhibitor **26** (magenta) overlaid with the inhibitor **1** (green)-bound crystal structure of HIV-1 protease.

227 **Conclusion**

228 A series of novel HIV protease inhibitors incorporating
 229 3-hydroxysalicylic acid-derived acyclic and cyclic
 230 P2 ligand has been designed, synthesized, and evalu-
 231 ated. The cyclic inhibitors incorporated 13–15-mem-
 232 bered macrocycles. In general, cyclic inhibitors are
 233 considerably more potent than their acyclic counterparts
 234 both in enzyme inhibitory and in antiviral assays.
 235 Inhibitors with 13–15-membered macrocyclic ligands
 236 have shown subnanomolar enzyme inhibitory potencies.
 237 The inhibitors contain only two stereocenters, and the
 238 cyclic inhibitors can be readily prepared by using a ring-
 239 closing olefin metathesis. The saturated 14-membered
 240 macrocycle **26** with the *para*-methoxybenzenesulfon-
 241 amide P₂' ligand displayed the highest enzyme inhibi-
 242 tory potency with a K_i value of 0.7 nM. This compound
 243 has also shown the best antiviral IC₅₀ value of 0.3 μM.
 244 Substitution of a 1,3[benzo]dioxolane sulfonamide for
 245 the *para*-methoxybenzenesulfonamide resulted in a
 246 noticeable attenuation of biological activity of the 14-
 247 membered macrocycle. Further design and chemical
 248 modifications of these inhibitors utilizing our structure-
 249 based design strategies are currently underway.

250 **Experimental Section**

251 **General.** ¹H and ¹³C NMR spectra were obtained in CDCl₃
 252 with an AM or Avance 400 Bruker instrument operating at
 253 400 MHz for ¹H and 100 MHz for ¹³C. Chemical shifts are
 254 reported in ppm, and coupling constants (*J*) are reported in
 255 Hertz. Optical rotations were measured using a Perkin-Elmer
 256 341 polarimeter using a sodium lamp (589 nm) in chloroform
 257 unless otherwise stated. Infrared spectra were measured using
 258 a Genesis II FTIR in chloroform as thin films using sodium
 259 chloride plates. Thin-layer chromatography (TLC) was per-
 260 formed on E. Merck silica gel 60-F-254 plates. Mass spectra
 261 were recorded on a Finnegan LCQ mass spectrometer as the
 262 value *m/z*. Flash chromatography was performed using 230–
 263 400 mesh silica gel. Tetrahydrofuran was distilled from
 264 sodium/benzophenone, and benzene, methylene chloride, *N,N*-
 265 dimethylformamide, and toluene were distilled from CaH₂
 266 under N₂.

267 **3-(*tert*-Butyl-dimethyl-silyloxy)-2-hydroxy-benzo-**
 268 **ic Acid Methyl Ester (5).** To a stirring solution of 1.51 g (9.8
 269 mmol) of 2,3 dihydroxybenzoic acid **4** in 35 mL of MeOH and
 270 7 mL of water was added 1.60 g (4.9 mmol) of CsCO₃. The
 271 solution was stirred at 23 °C for 30 min and then concentrated.
 272 Absolute ethanol (3 × 4 mL) was added, the solution was
 273 reconstituted to remove water, and the crude product was
 274 dried under vacuum. The resulting brown solid was dissolved
 275 in 10 mL of DMF, and the solution was cooled to 0 °C. Methyl
 276 iodide (0.64 mL, 10.3 mmol) was added, and after the solution
 277 was warmed to 23 °C, stirring was continued in the dark for
 278 13 h. Water (40 mL) and EtOAc (70 mL) were added, and the

279 layers were separated. The organic layer was then washed
 280 with water (3 × 40 mL) and then 40 mL of brine. The organic
 281 layer was dried over Na₂SO₄, filtered, and concentrated. The
 282 residue was purified by flash silica gel chromatography (5–
 283 20% EtOAc/hexanes) to provide the methyl ester as a pale
 284 yellow solid (1.33 g, 81%); mp 78–78.5 °C. IR (neat): 3463,
 285 1675 cm⁻¹. ¹H NMR (400 MHz, CDCl₃): δ 10.90 (s, 1 H), 7.36
 286 (dd, 1 H, *J* = 1.7, 8.2 Hz), 7.11 (dd, 1 H, *J* = 1.3, 8.0 Hz), 6.80
 287 (t, 1 H, *J* = 7.9 Hz), 5.71 (s, 1 H), 3.95 (s, 3H). ¹³C NMR (100
 288 MHz, CDCl₃): δ 170.8, 148.8, 145.0, 120.6, 119.8, 119.2, 112.4,
 289 52.5.

290 To a stirring solution of above ester (1.28 g, 7.6 mmol) in 6
 291 mL of DMF at 0 °C was added 1.25 g (8.3 mmol) of TBDMSCl
 292 and 1.8 mL (10.3 mmol) of *N,N*-diisopropylethylamine. Stirring
 293 was continued at 0 °C for 20 min, and then, 35 mL of water
 294 and 45 mL of EtOAc were added. The layers were separated,
 295 and the organic layer was washed with 35 mL of water and
 296 20 mL of brine, dried over Na₂SO₄, filtered, and concentrated.
 297 Purification by flash silica gel chromatography (hexanes to 5%
 298 EtOAc/hexanes) provided **5** as a yellow oil (2.07 g) 96%. IR
 299 (neat): 3173, 1679 cm⁻¹. ¹H NMR (500 MHz, CDCl₃): δ 10.76
 300 (s, 1 H), 7.45 (dd, 1 H, *J* = 1.6, 8.1 Hz), 7.03 (dd, 1 H, *J* = 1.5,
 301 8.0 Hz), 6.73 (t, 1 H, *J* = 8.0 Hz), 3.94 (s, 3 H), 1.01 (s, 9 H),
 302 0.20 (s, 6 H). ¹³C NMR (125 MHz, CDCl₃): δ 171.3, 154.3,
 303 144.9, 126.7, 122.7, 118.9, 113.6, 52.7, 26.1, 18.9, -4.2.

304 **2-Allyloxy-3-(*tert*-butyl-dimethyl-silyloxy)benzoic**
 305 **Acid Methyl Ester (6).** To a stirring solution of **5** (101 mg,
 306 0.36 mmol) in 4 mL of THF was added 60 μL (0.381 mmol) of
 307 DEAD, 26 μL (0.382 mmol) of allyl alcohol, and 99.5 mg (0.379
 308 mmol) of PPh₃. The solution was stirred at 23 °C for 3 h and
 309 then concentrated. Purification by flash silica gel chromatog-
 310 raphy (0.3–5% EtOAc/hexanes) provided the product **6** as a
 311 yellow oil in 58% yield. IR (neat): 2952, 1733, 1470 1299, 1020,
 312 934, 836 cm⁻¹. ¹H NMR (500 MHz, CDCl₃): δ 7.37 (m, 1 H),
 313 7.00 (m, 2 H), 6.11 (dddd, 1 H, *J* = 5.9, 5.9, 10.5, 17.2 Hz),
 314 5.35 (ddd, 1 H, *J* = 1.6, 3.2, 17.2 Hz), 5.23 (ddd, 1 H, *J* = 1.2,
 315 2.7, 10.4 Hz), 4.53 (ddd, 2 H, *J* = 1.2, 1.3, 5.9 Hz), 3.88 (s, 3
 316 H), 1.01 (s, 9 H), 0.19 (s, 6 H). ¹³C NMR (125 MHz, CDCl₃): δ
 317 167.3, 150.4, 150.3, 134.5, 127.2, 125.3, 124.3, 124.0, 118.1,
 318 74.8, 52.6, 26.1, 18.7, -4.1.

319 **2-But-3-enyloxy-3-(*tert*-butyl-dimethyl-silyloxy)ben-**
 320 **zoic Acid Methyl Ester (7).** To a stirred solution of **5** (201
 321 mg, 0.71 mmol) in 3 mL of THF with stirring was added 0.13
 322 mL (0.83 mmol) of DEAD, 74 μL (0.86 mmol) of 3-buten-1-ol,
 323 and 226 mg (0.86 mmol) of PPh₃. The solution was stirred for
 324 5 h and then concentrated. The crude product was purified by
 325 flash silica gel chromatography (0.5–4% EtOAc/hexanes) to
 326 give pure **7** as a yellow oil in 63% yield. IR (neat): 1734 cm⁻¹.
 327 ¹H NMR (500 MHz, CDCl₃): δ 7.34 (m, 1 H), 6.99 (m, 2 H),
 328 5.88 (tdd, 1 H, *J* = 10.3, 13.6, 17.2 Hz), 5.13 (ddd, 1 H, *J* =
 329 1.6, 3.2, 17.2 Hz), 5.06 (dd, 1 H, *J* = 1.5, 10.3 Hz), 4.05 (t, 2 H,
 330 *J* = 7.2 Hz), 3.89 (s, 3 H), 2.55 (m, 2 H), 1.01 (s, 9 H), 0.2 (s,
 331 6 H). ¹³C NMR (100 MHz, CDCl₃): δ 167.3, 150.5, 150.2, 135.1,
 332 127.1, 125.1, 124.1, 123.9, 117.1, 73.2, 52.5, 34.9, 26.1, 18.7,
 333 -4.0.

334 **3-(*tert*-Butyl-dimethyl-silyloxy)-2-pent-4-enyloxy-**
 335 **benzoic Acid Methyl Ester (8).** Etherification of **5** with

336 4-penten-1-ol following the procedure for **6** provided 160 mg
337 of **8** in 89% yield as a colorless oil. IR (neat): 1733 cm^{-1} . ^1H
338 NMR (500 MHz, CDCl_3): δ 7.33 (dd, 1 H, $J = 2.9, 6.6$ Hz),
339 6.98 (m, 2 H), 5.86 (tdd, 1 H, $J = 6.6, 10.3, 17.2$ Hz), 5.04 (ddd,
340 1 H, $J = 1.6, 3.4, 17.1$ Hz), 4.97 (dd, 1 H, $J = 1.6, 10.2$ Hz),
341 4.01 (t, 2 H, $J = 7.0$ Hz), 3.89 (s, 3 H), 2.19 (m, 2 H), 1.89 (m,
342 2 H), 1.01 (s, 9 H), 0.20 (s, 6 H). ^{13}C NMR (125 MHz, CDCl_3):
343 δ 167.4, 150.7, 150.2, 138.7, 127.1, 125.1, 124.0, 123.8, 115.1,
344 73.8, 52.5, 30.6, 29.7, 26.1, 18.7, -4.0.

345 **2-Allyloxy-3-hydroxy-benzoic Acid (9)**. To a stirring
346 solution of 113 mg of **6** in 4 mL of THF at 0 $^\circ\text{C}$ was added 0.56
347 mL of TBAF (1 M THF) dropwise under N_2 . Stirring
348 was continued at 0 $^\circ\text{C}$ for about 10 min after which time 10 mL of
349 saturated NH_4Cl solution, 4 mL of water, and 15 mL of EtOAc.
350 The layers were separated, and the organic layer was washed
351 with 15 mL of water and then 15 mL of brine, dried over Na_2SO_4 ,
352 filtered, and concentrated. Purification by flash silica gel
353 chromatography (2–5% EtOAc/hexanes) resulted in 56.2 mg
354 (0.349 mmol) of the corresponding methyl ester in 77% yield
355 as a colorless oil. IR (neat): 3420, 2952, 1722, 1466, 1284, 988,
356 755 cm^{-1} . ^1H NMR (500 MHz, CDCl_3): δ 7.41 (dd, 1 H, $J =$
357 1.7, 7.9 Hz), 7.15 (dd, 1 H, $J = 1.7, 8.1$ Hz), 7.06 (t, 1 H, $J =$
358 8.0 Hz), 6.10 (qdd, 1 H, $J = 6.0, 6.1, 10.4$ Hz), 5.96 (s, 1 H),
359 5.43 (m, 1 H), 5.32 (dd, 1 H, $J = 0.69, 10.3$ Hz), 4.53 (d, 2 H,
360 $J = 6.1$ Hz), 3.91 (s, 3 H). ^{13}C NMR (125 MHz, CDCl_3): δ 166.3,
361 150.4, 146.2, 133.6, 124.9, 124.2, 123.2, 119.9, 119.8, 76.6, 52.7.

362 A mixture of the above ester (30.7 mg, 0.15 mmols) and 32.7
363 mg (0.78 mmols) of LiOH in 2 mL of THF and 2 mL of water
364 was stirred at 55 $^\circ\text{C}$ for 2.5 h. Heating was stopped, and 2 mL
365 of 1 N HCl, 2 mL of water, and 8 mL of EtOAc were added.
366 After the layers were separated, the organic layer was washed
367 with 5 mL of brine, dried over sodium sulfate, filtered, and
368 concentrated. Purification by flash silica gel chromatography
369 of the crude product resulted in 23.6 mg of acid **9** in 83% yield
370 as a colorless solid; mp 101.5–103.5 $^\circ\text{C}$. IR (neat): 3162, 1703,
371 1417, 1295, 1210, 944, 747 cm^{-1} . ^1H NMR (500 MHz, CDCl_3):
372 δ 7.62 (dd, 1 H, $J = 1.7, 7.9$ Hz), 7.20 (dd, 1 H, $J = 1.7, 8.0$
373 Hz), 7.13 (t, 1 H, $J = 8.0$), 6.13 (tdd, 1 H, $J = 6.2, 10.5, 16.9$
374 Hz), 5.46 (m, 1 H), 5.38 (dd, 1 H, $J = 0.6, 9.7$ Hz), 4.64 (d, 2 H,
375 $J = 6.2$ Hz). ^{13}C NMR (125 MHz, CDCl_3): δ 167.5, 149.8, 146.2,
376 132.6, 125.6, 124.5, 123.1, 121.7, 121.2, 76.9.

377 **2-But-3-enyloxy-3-hydroxy-benzoic Acid (10)**. To 129
378 mg (0.38 mmol) of **7** in 3 mL of THF at 0 $^\circ\text{C}$ with stirring was
379 added slowly 0.6 mL of TBAF (1 M THF). After 20 min, 10
380 mL of saturated NH_4Cl solution, 2 mL of water, and 15 mL of
381 EtOAc were added. The organic layer was washed with 10 mL
382 of brine, dried over Na_2SO_4 , filtered, and concentrated. Purifi-
383 cation by flash silica gel chromatography (5–10% EtOAc/
384 hexanes) gave 65 mg of the corresponding diol in 77% yield as
385 a colorless oil. IR (neat): 3443, 1726 cm^{-1} . ^1H NMR (400 MHz,
386 CDCl_3): δ 7.39 (dd, 1 H, $J = 1.7, 7.7$ Hz), 7.13 (dd, 1 H, $J =$
387 1.7, 8.1 Hz), 7.04 (t, 1 H, $J = 8.0$ Hz), 6.08 (s, 1 H), 5.95 (tdd,
388 1 H, $J = 6.9, 10.2, 17.2$ Hz), 5.30 (ddd, 1 H, $J = 1.5, 2.8, 16.9$
389 Hz), 5.24 (dd, 1 H, $J = 1.1, 9.7$ Hz), 4.08 (t, 2 H, $J = 6.1$ Hz),
390 3.92 (s, 3 H), 2.55 (m, 2 H). ^{13}C NMR (100 MHz, CDCl_3): δ
391 166.4, 150.4, 146.5, 135.3, 124.8, 124.0, 123.1, 119.9, 119.0,
392 74.5, 52.6, 35.0.

393 A mixture of above diol (61 mg, 0.28 mmol) and 79 mg (1.9
394 mmols) of LiOH in 2 mL of THF and 2 mL of water was heated
395 at 55 $^\circ\text{C}$. After 2 h, 2 mL of 1 N HCl and 15 mL of EtOAc. The
396 layers were separated, and the organic layer was washed with
397 10 mL of brine, dried over Na_2SO_4 , filtered, and concentrated.
398 Purification by flash silica gel chromatography (10% MeOH/
399 CH_2Cl_2) provided **10** in 94% yield (54 mg) as a white solid; mp
400 70–73 $^\circ\text{C}$. IR (neat): 3177, 1716 cm^{-1} . ^1H NMR (400 MHz,
401 CHCl_3): δ 7.58 (d, 1 H, $J = 7.7$ Hz), 7.19 (d, 1 H, $J = 7.9$ Hz),
402 7.11 (t, 1 H, $J = 7.9$ Hz), 5.95 (m, 1 H), 5.29 (m, 2 H), 4.17 (t,
403 2 H, $J = 6.1$ Hz), 2.58 (m, 2 H). ^{13}C NMR (100 MHz, CHCl_3) δ
404 168.9, 149.7, 146.4, 134.4, 124.9, 123.8, 122.4, 121.1, 119.0,
405 74.5, 34.4.

406 **3-Hydroxy-2-pent-4-enyloxy-benzoic Acid (11)**. A mix-
407 ture of 160 mg (0.45 mmol) of **8** and 111 mg (2.64 mmol) of
408 LiOH in 6 mL of THF and 2 mL of water was stirred at 23 $^\circ\text{C}$
409 for about 2 h and then at 50 $^\circ\text{C}$ for 12.5 h. Heating was

410 stopped, and 1 N HCl was added to a pH of 1 followed by 12
411 mL of EtOAc. The layers were separated, and the organic layer
412 was washed with 5–6 mL of brine, dried over Na_2SO_4 , filtered,
413 and concentrated. Purification by flash silica gel chromatog-
414 raphy (20–50% EtOAc/hexanes) gave pure product **11** as a
415 white amorphous solid; 89 mg in 88% yield; mp 70–74 $^\circ\text{C}$. IR
416 (neat): 3082, 1702 cm^{-1} . ^1H NMR (500 MHz, CHCl_3): δ 7.58
417 (dd, 1 H, $J = 1.6, 7.9$ Hz), 7.21 (dd, 1 H, $J = 1.5, 8.1$ Hz), 7.09
418 (t, 1 H, $J = 8.0$ Hz), 5.87 (tdd, 1 H, $J = 6.7, 10.3, 17.1$ Hz),
419 5.04 (dd, 2 H, $J = 1.4, 10.2$ Hz), 4.13 (t, 2 H, $J = 6.6$ Hz), 2.27
420 (q, 2 H, $J = 7.1$ Hz), 1.97 (quint, 2 H, $J = 7.0$ Hz). ^{13}C NMR
421 (125 MHz, CDCl_3): δ 169.9, 150.1, 146.9, 138.1, 125.2, 124.2,
422 122.8, 121.8, 116.1, 75.6, 30.5, 29.5.

423 **(E)-Nona-2,8-dien-1-ol (13)**. To a stirring solution of diol
424 **12** (1.36 g, 9.5 mmol) in 10 mL of THF and 1 mL of water was
425 added 5.29 g (24.7 mmol) of NaIO_4 . The resulting white
426 mixture was stirred at 23 $^\circ\text{C}$ for about 30 min. The mixture
427 was dried with Na_2SO_4 , filtered through Celite, and concen-
428 trated. The resulting aldehyde was again dried with Na_2SO_4 ,
429 concentrated, and used without further purification for the
430 next reaction.

431 To a stirring solution of triethylphosphonoacetate (2.43 g,
432 10.8 mmols) in 6 mL of THF at 0 $^\circ\text{C}$ was added 436 mg of
433 NaH (60% dispersion in mineral oil). After 20 min, the above
434 aldehyde was added in 6 mL of THF, and the solution was
435 allowed to warm to 23 $^\circ\text{C}$. After 15 min, the reaction was
436 quenched with about 2 mL of saturated NH_4Cl solution and 1
437 mL of water. Diethyl ether (15 mL) was added, and the layers
438 were separated. The organic layer was washed with 10 mL of
439 brine, dried over Na_2SO_4 , filtered, and concentrated. Purifica-
440 tion (flash silica gel chromatography-hexanes to 2% EtOAc/
441 hexanes) gave the corresponding α,β -unsaturated ester (1.36
442 g, 79%) as a pale yellow liquid. IR (neat): 1722, 1654 cm^{-1} .
443 ^1H NMR (400 MHz, CDCl_3): δ 6.96 (ddd, 1 H, $J = 6.9, 7.0,$
444 15.6 Hz), 5.80 (m, 2 H), 5.00 (ddd, 1 H, $J = 1.6, 3.2, 17.0$ Hz),
445 4.95 (dd, 1 H, $J = 1.1, 9.7$ Hz), 4.18 (q, 2 H, $J = 7.1$ Hz), 2.20
446 (m, 2 H), 2.06 (q, 2 H, $J = 7.0$ Hz), 1.45 (m, 4 H), 1.29 (t, 3 H,
447 $J = 7.2$ Hz). ^{13}C NMR (400 MHz, CDCl_3): δ 166.8, 149.2, 138.6,
448 121.3, 114.6, 60.1, 33.5, 32.0, 28.3, 27.4, 14.3.

449 To a stirred solution of the above ester (1.32 g, 7.2 mmol)
450 in 20 mL of CH_2Cl_2 at -78 $^\circ\text{C}$ was added 17 mL of DIBAL-H
451 (1 M hexanes). After it was stirred at -78 $^\circ\text{C}$ for 20 min, 20
452 mL of EtOAc and 40 mL of 1 N HCl were added, and after
453 this mixture was warmed to 23 $^\circ\text{C}$, 140 mL of 1 N HCl and 20
454 mL of CH_2Cl_2 were added. The layers were separated, dried
455 over Na_2SO_4 , filtered, and concentrated. Purification by flash
456 silica gel chromatography (10% EtOAc/hexanes) provided **13**
457 as a pale yellow liquid in 90% yield (910 mg). IR (neat): 3336
458 cm^{-1} . ^1H NMR (400 MHz, CDCl_3): δ 5.81 (tdd, 1 H, $J = 6.7,$
459 10.3, 17.3), 5.66 (dtd, 2 H, $J = 5.8, 15.3, 20.2$), 5.00 (ddd, 1 H,
460 $J = 1.7, 3.4, 16.9$ Hz), 4.93 (m, 1 H), 4.08 (d, 2 H, $J = 5.1$ Hz),
461 2.05 (m, 4 H), 1.39 (m, 4 H), 1.31 (s, 1 H). ^{13}C NMR (100 MHz,
462 CDCl_3): δ 138.9, 133.3, 129.0, 114.4, 63.8, 33.6, 32.0, 28.6, 28.4.

463 **(2R,3R)-(3-Hex-5-enyl-oxiranyl)methanol (14)**. A 125
464 mL reaction flask with 183 mg of 4 A molecular sieves powder
465 was flame-dried and cooled under vacuum. To the flask was
466 added 20 mL of CH_2Cl_2 , followed by 0.10 mL (0.34 mmol) of
467 $\text{Ti}(\text{O}^i\text{Pr})_4$ and 60 μL (0.055 mmol) of (-)-DET. The resulting
468 solution was cooled to -20 $^\circ\text{C}$, and 2.0 mL of *tert*-butyl
469 hydroperoxide (5–6 M decane) was added dropwise. After 45
470 min, 0.887 g (6.3 mmol) of **13** in 10 mL of CH_2Cl_2 was added
471 and stirring was continued at -20 $^\circ\text{C}$ for 3 h and was aged in
472 a refrigerator for 11 h at about -20 $^\circ\text{C}$. The solution mixture
473 was warmed to 0 $^\circ\text{C}$, and 3 mL of water was added. After 30
474 min, a 30% NaOH/brine solution was added, and the mixture
475 was warmed to 23 $^\circ\text{C}$. After 1 h, 20 mL of CH_2Cl_2 was added,
476 and the layers were separated. The aqueous layer was
477 extracted with 10 mL of CH_2Cl_2 , and the combined extracts
478 were dried over Na_2SO_4 . Purification by flash silica gel
479 chromatography (20–25% EtOAc/hexanes) gave 0.798 g of **14**
480 in 78% yield as a pale yellow liquid: $[\alpha]_D^{25} +34.2$ (c 0.30,
481 CHCl_3). IR (neat): 3400, 1026 cm^{-1} . ^1H NMR (400 MHz,
482 CDCl_3): δ 5.80 (tdd, 1 H, $J = 6.8, 10.3, 17.1$ Hz), 5.00 (ddd, 1
483 H, $J = 1.7, 3.5, 17.2$ Hz), 4.95 (dd, 1 H, $J = 1.0, 9.5$ Hz), 3.91

484 (ddd, 1 H, $J = 2.6, 5.6, 12.5$ Hz), 3.63 (m, 1 H), 2.96 (ddd, 1 H,
485 $J = 2.4, 5.5, 5.7$ Hz), 2.92 (ddd, 1 H, $J = 2.1, 2.5, 4.5$ Hz), 2.06
486 (m, 2 H), 1.8 (m, 1 H), 1.57 (m, 2 H), 1.46 (m, 4 H). ^{13}C NMR
487 (100 MHz, CDCl_3): δ 138.6, 114.6, 61.6, 58.4, 55.9, 33.6, 31.4,
488 28.6, 25.4.

489 **(2S,3S)-3-Azido-non-8-ene-1,2-diol (15)**. A solution of 1.5
490 mL (5.1 mmol) of $\text{Ti}(\text{O}^i\text{Pr})_4$ and 1.2 mL (9.0 mmol) of TMSN_3
491 in 20 mL of benzene was heated at 90 °C for 4 h. To the heating
492 yellow solution was added 0.77 g (4.9 mmol) of **14** in 5 mL of
493 benzene, and reflux was continued for 20 min. The solution
494 was then cooled to 0 °C, 40 mL of 15% H_2SO_4 solution was
495 added, and the mixture was stirred vigorously for 1 h. The
496 layers were separated, and the organic layer was washed with
497 20 mL of saturated NaHCO_3 solution, then with 20 mL of
498 brine, dried over Na_2SO_4 , filtered, and concentrated. Purifica-
499 tion by flash silica gel chromatography (40% EtOAc/hexanes)
500 provided **15** as a yellow oil in 100% yield (0.97 g): $[\alpha]_D^{25} +13.2$
501 (c 0.49, CHCl_3). IR (neat): 3077, 2101 cm^{-1} . ^1H NMR (400
502 MHz, CDCl_3): δ 5.80 (ddd, 1 H, $J = 6.6, 10.1, 16.8$ Hz), 4.99
503 (m, 2 H), 3.72 (m, 3 H), 3.46 (m, 1 H), 2.80 (s, 1 H), 2.09 (m, 3
504 H), 1.54 (m, 6 H). ^{13}C NMR (100 MHz, CDCl_3): δ 138.5, 114.7,
505 73.5, 64.6, 63.1, 33.5, 30.4, 28.6, 25.7. MS-ESI (m/z): 222.2
506 ($\text{M} + \text{Na}$) $^+$.

507 **(1S,2R)-2'-(1-Azido-hept-6-enyl)oxirane (16)**. A clear
508 solution of (960 mg, 4.8 mmol) of **15** and 1-chlorocarbonyl-
509 methylethyl acetate (0.9 mL, 0.62 mmol) in 10 mL of CHCl_3
510 was stirred at 23 °C for 15 min. Saturated NaHCO_3 solution
511 was added, and the mixture was stirred for 10 min. The layers
512 were separated, and the organic layer was dried over Na_2SO_4 ,
513 filtered, and concentrated. The crude product was used directly
514 for the next reaction without further purification.

515 A mixture of the above crude product and NaOMe (0.37 g,
516 6.8 mmol) in 10 mL of THF was stirred at 23 °C for 3 h. To
517 the mixture was added 6 mL of saturated NH_4Cl solution, 2
518 mL of water, and 20 mL of EtOAc. The layers were separated,
519 and the organic layer was dried over Na_2SO_4 , filtered, and
520 concentrated. The crude product was purified by flash silica
521 gel chromatography (5% EtOAc/hexanes) to give 2.60 g and
522 54% yield of **16** as a yellow oil: $[\alpha]_D^{25} +5.9$ (c 0.32, CHCl_3). IR
523 (neat): 2101 cm^{-1} . ^1H NMR (400 MHz, CDCl_3): δ 5.80 (tdd, 1
524 H, $J = 6.7, 10.3, 17.2$ Hz), 4.99 (m, 2 H), 3.32 (m, 1 H), 3.01
525 (m, 1 H), 2.80 (m, 2 H), 2.08 (m, 2 H), 1.80–1.41 (m, 6 H). ^{13}C
526 NMR (100 MHz, CDCl_3): δ 138.5, 114.7, 62.5, 53.4, 44.9, 33.5,
527 31.7, 28.6, 25.2.

528 **(2R,3S)-N-(3-Azido-2-hydroxy-non-8-enyl)-N-isobutyl-
529 4-methoxy-benzenesulfonamide (17)**. A solution of **16** (0.45
530 g, 2.5 mmol) and isopropylamine (0.41 mL, 4.1 mmol) in 5 mL
531 of $i\text{PrOH}$ was stirred at 90 °C for 80 min. After this period,
532 the reaction mixture was concentrated. The residue was
533 purified by flash silica gel chromatography (60–80% EtOAc/
534 hexanes) to provide the corresponding amine as a yellow oil
535 (0.38 g, 62%): $[\alpha]_D^{25} +2.0$ (c 0.45, CHCl_3). IR (neat): 3323,
536 2100 cm^{-1} . ^1H NMR (500 MHz, CDCl_3): δ 5.80 (tdd, 1 H, $J =$
537 6.7, 10.3, 17.1 Hz), 5.01 (ddd, 1 H, $J = 1.6, 3.4, 17.1$ Hz), 4.95
538 (dd, 1 H, $J = 1.8, 10.1$ Hz), 3.58 (ddd, 1 H, $J = 3.7, 5.3, 12.6$
539 Hz), 3.39 (m, 1 H), 2.77 (dd, 1 H, $J = 3.6, 12.1$ Hz), 2.64 (dd,
540 1 H, $J = 8.9, 12.1$ Hz), 2.43 (ddd, 3 H, $J = 6.8, 9.0, 11.7$ Hz),
541 2.07 (dd, 2 H, $J = 7.0$ Hz), 1.72 (octet, 1 H, $J = 6.7$ Hz), 1.63–
542 1.51 (m, 2 H), 1.51–1.40 (m, 5 H), 0.92 (d, 3 H, $J = 2.1$ Hz),
543 0.91 (d, 3 H, $J = 2.1$ Hz). ^{13}C NMR (125 MHz, CDCl_3): δ 139.0,
544 115.0, 71.3, 66.1, 58.0, 50.8, 34.0, 30.8, 29.0, 28.9, 26.3, 20.9.

545 A mixture of above amine (88 mg, 0.34 mmol) and 4-methoxy-
546 benzenesulfonyl chloride (70.9 mg, 0.34 mmol) in a mixture
547 (1:1) of CH_2Cl_2 and saturated NaHCO_3 solution (10 mL) was
548 stirred at 23 °C. After 12.5 h, 10 mL of CH_2Cl_2 was added,
549 and the layers were separated. The aqueous layer was
550 extracted with 10 mL of CH_2Cl_2 . The combined extracts were
551 dried over Na_2SO_4 , filtered, and concentrated. The crude
552 product was purified by flash silica gel chromatography to give
553 **17** (132 mg, 90%) as a clear oil: $[\alpha]_D^{25} -19.6$ (c 0.5, CHCl_3).
554 IR (neat): 3498, 2101, 1597, 1335 cm^{-1} . ^1H NMR (400 MHz,
555 CDCl_3): δ 7.76 (dd, 1 H, $J = 3.0, 9.9$ Hz), 7.75 (dd, 1 H, $J =$
556 2.0, 7.0 Hz), 7.02 (dd, 1 H, $J = 2.9, 10.1$ Hz), 7.01 (dd, 1 H, J
557 = 1.7, 7.2 Hz), 5.80 (tdd, 1 H, $J = 6.7, 10.3, 17.0$ Hz), 5.01 (dd,

558 1 H, $J = 1.6, 17.2$ Hz), 4.96 (d, 1 H, $J = 10.4$ Hz), 3.88 (s, 3 H),
559 3.78 (m, 1 H), 3.47 (d, 1 H, $J = 3.1$ Hz), 3.34 (ddd, 1 H, $J =$
560 3.7, 5.5, 8.7 Hz), 3.21 (dd, 1 H, $J = 9.4, 15.3$ Hz), 3.02 (m, 2
561 H), 2.81 (dd, 1 H, $J = 6.5, 13.3$ Hz), 2.08 (q, 2 H, $J = 6.8$ Hz),
562 1.85 (m, 1 H), 1.65 (m, 1 H), 1.60–1.42 (m, 5 H), 0.96 (d, 3 H,
563 $J = 6.6$ Hz), 0.90 (d, 3 H, $J = 6.6$ Hz). ^{13}C NMR (100 MHz,
564 CDCl_3): δ 163.1, 138.5, 129.7, 129.5, 114.7, 114.4, 72.4, 65.4,
565 58.9, 55.6, 52.7, 33.5, 30.3, 28.6, 27.2, 25.6, 20.2, 19.8. MS-
566 ESI (m/z): 425.2 ($\text{M} + \text{H}$) $^+$.

567 **(2R,3S)-N-(3-Amino-2-hydroxy-non-8-enyl)-N-isobutyl-
568 4-methoxy-benzenesulfonamide (18)**. To a stirred suspen-
569 sion of LiAlH_4 (20 mg, 0.25 mmol) in 5 mL of THF was added
570 **17** (110 mg, 0.24 mmol) in 5 mL of THF. Stirring was
571 continued for 50 min, and the reaction was quenched by adding
572 successively 20 μL of water, 20 μL of 15% NaOH , and 60 μL of
573 brine. The mixture was filtered through Celite and concen-
574 trated. The resulting product **18** was used in the next reaction
575 without further purification. IR (neat): 3351, 1596, 1333 cm^{-1} .
576 ^1H NMR (400 MHz, CDCl_3): δ 7.75 (dd, 1 H, $J = 2.9, 11.7$
577 Hz), 7.74 (dd, 1 H, $J = 1.7, 7.1$ Hz), 6.98 (dd, 1 H, $J = 2.9,$
578 11.8 Hz), 6.97 (dd, 1 H, $J = 1.9, 7.1$ Hz), 5.79 (tdd, 1 H, $J =$
579 6.6, 10.2, 17.2 Hz), 5.02 (ddd, 1 H, $J = 1.6, 3.3, 17.0$ Hz), 4.94
580 (m, 1 H), 3.87 (s, 3 H), 3.70 (m, 1 H), 3.25 (dd, 1 H, $J = 9.3,$
581 15.0 Hz), 3.04 (m, 2 H), 2.85 (m, 2 H), 2.06 (dd, 2 H, $J = 6.7,$
582 13.5 Hz), 1.90 (m, 2 H), 1.50–1.30 (m, 5 H), 1.43 (m, 3 H),
583 0.94 (d, 3 H, $J = 6.5$ Hz), 0.90 (d, 3 H, $J = 6.5$ Hz). ^{13}C NMR
584 (125 MHz, CDCl_3): δ 163.3, 139.1, 130.7, 129.9, 115.0, 114.7,
585 73.6, 58.9, 56.0, 54.8, 52.4, 34.1, 33.1, 29.3, 27.6, 26.3, 20.6,
586 20.3.

587 **(1'S,1'R)-2-Allyloxy-3-hydroxy-N-(1'-{1''-hydroxy-2''-
588 [isobutyl-(4-methoxy-benzenesulfonyl)amino]ethyl}hept-
589 6'-enyl)benzamide (19)**. To a stirring solution of acid **9** (23.9
590 mg, 0.12 mmol) in 2 mL of DMF at 0 °C was added EDC (30.1
591 mg, 0.16 mmol), HOBT (22.2 mg, 0.16 mmol), 50.8 mg (0.127
592 mmol) of amine **18** in 2 mL of DMF, and 86 μL (0.62 mmol) of
593 Et_3N . The solution was allowed to warm to 23 °C, and stirring
594 was continued for 19 h. To the solution was then added 4 mL
595 of water and 20 mL of EtOAc. The layers were separated, and
596 the organic layer was washed with 10 mL of water and 10 mL
597 of brine, dried over Na_2SO_4 , filtered, and concentrated. Flash
598 silica gel chromatography yielded **19** (35.1 mg, 50%) as an oil:
599 $[\alpha]_D^{25} -12.5$ (c 0.12, CHCl_3). IR (neat): 3347, 2926, 1638, 1577,
600 1534, 1497, 1463, 1334, 1260, 1151, 1091, 807, 757 cm^{-1} . ^1H
601 NMR (400 MHz, CDCl_3): δ 7.70 (m, 3 H), 7.52 (dd, 1 H, $J =$
602 2.8, 6.7 Hz), 7.12 (m, 2 H), 6.96 (d, 2 H, $J = 8.9$ Hz), 6.11 (m,
603 1 H), 5.77 (tdd, 1 H, $J = 6.6, 10.3, 17.1$ Hz), 5.64 (s, 1 H), 5.48
604 (d, 1 H, $J = 17.1$ Hz), 5.37 (d, 1 H, $J = 10.5$ Hz), 4.97 (dd, 1 H,
605 $J = 1.6, 15.5$ Hz), 4.92 (d, 1 H, $J = 10.4$ Hz), 4.55 (dd, 1 H, $J =$
606 5.8, 12.4 Hz), 4.45 (dd, 1 H, $J = 5.8, 12.4$ Hz), 4.10 (m, 1 H),
607 3.93 (dd, 1 H, $J = 3.2, 9.1$ Hz), 3.87 (s, 3 H), 3.78 (d, 1 H, $J =$
608 3.4 Hz), 3.18 (dd, 1 H, $J = 9.0, 15.2$ Hz), 3.04 (d, 1 H, $J = 2.4$
609 Hz), 2.98 (dd, 1 H, $J = 8.4, 13.4$ Hz), 2.84 (dd, 1 H, $J = 6.8,$
610 13.3 Hz), 2.04 (m, 2 H), 1.86 (m, 1 H), 1.63 (m, 2 H), 1.44 (m,
611 2 H), 1.38 (m, 2 H), 0.91 (d, 3 H, $J = 6.6$ Hz), 0.86 (d, 3 H, $J =$
612 6.5 Hz). ^{13}C NMR (125 MHz, CDCl_3): δ 165.8, 163.4, 149.6,
613 144.0, 139.1, 132.7, 130.4, 129.9, 127.3, 125.8, 122.9, 120.2,
614 119.6, 115.0, 114.7, 76.3, 73.5, 58.9, 56.0, 54.0, 53.4, 34.0, 30.1,
615 29.5, 29.3, 27.6, 26.1, 20.5, 20.3. HRMS-ESI (m/z): ($\text{M} + \text{Na}$) $^+$
616 calcd for $\text{C}_{30}\text{H}_{42}\text{N}_2\text{O}_7\text{NaS}$, 574.2713; found, 574.2792.

617 **(1'S,1'R)-2-But-3'-enyloxy-3-hydroxy-N-(1'-{1''-hy-
618 droxy-2''-[isobutyl-(4-methoxy-benzenesulfonyl)amino]-
619 ethyl}hept-6'-enyl)benzamide (20)**. To a stirring solution
620 of **52** mg (0.12 mmol) of amine **18** in 2 mL of DMF at 0 °C was
621 added 25 mg (0.13 mmol) of EDC, 16 mg (0.12 mmol) of HOBT,
622 20 mg (0.096 mmol) of acid **10** in 2 mL of DMF, and finally 66
623 μL (0.47 mmol) of triethylamine. The mixture was allowed to
624 warm to 23 °C, and stirring was continued for 9 h. Water (5
625 mL) and EtOAc (20 mL) were added, and the layers were
626 separated. The organic layer was washed with 5 mL of water
627 and 6 mL of brine, dried over Na_2SO_4 , filtered, and concen-
628 trated. Purification by flash silica gel chromatography (40%
629 EtOAc/hexanes) provided **20** (34.1 mg) as an oil (61%): $[\alpha]_D^{25}$
630 -12.9 (c 0.19, CHCl_3). IR (neat): 3339, 1638, 1577, 1535, 1334
631 cm^{-1} . ^1H NMR (500 MHz, CDCl_3): δ 7.73 (m, 3 H), 7.48 (dd, 1

- 632 H, $J = 2.3, 7.3$ Hz), 7.10 (m, 2 H), 6.98 (dd, 1 H, $J = 2.9, 11.9$
633 Hz), 6.97 (dd, 1 H, $J = 2.0, 6.9$ Hz), 5.96 (tdd, 1 H, $J = 6.9,$
634 10.2, 17.2 Hz), 5.83 (s, 1 H) 5.77 (tdd, 1 H, $J = 6.7, 10.3, 17.1,$
635 Hz), 5.33 (m, 1 H), 5.29 (d, 1 H, $J = 10.2$ Hz), 4.97 (ddd, 1 H,
636 $J = 1.7, 3.5, 17.0$ Hz), 4.91 (m, 1 H), 4.09 (m, 2 H), 3.95 (m, 2
637 H), 3.87 (s, 3 H), 3.80 (d, 1 H, $J = 3.2,$ Hz), 3.21 (dd, 1 H, $J =$
638 9.1, 15.1 Hz), 3.01 (m, 1 H), 2.98 (dd, 1 H, $J = 2.9, 5.6$ Hz),
639 2.83 (dd, 1 H, $J = 6.6, 13.3$ Hz), 2.57 (m 2 H), 2.04 (m, 2 H),
640 1.86 (m, 1 H), 1.60 (m, 2 H), 1.45 (m, 2 H), 1.38 (m, 2 H), 0.91
641 (d, 3 H, $J = 6.6$ Hz), 0.86 (d, 3 H, $J = 6.6$ Hz). ^{13}C NMR (125
642 MHz, CDCl_3): δ 165.9, 163.5, 149.6, 144.3, 139.1, 134.6, 130.3,
643 129.9, 127.3, 125.8, 122.6, 119.7, 119.5, 115.0, 114.8, 74.8, 73.5,
644 59.1, 56.0, 54.1, 53.2, 34.6, 34.0, 30.1, 29.3, 27.6, 26.1, 20.5,
645 20.3. MS-ESI (m/z): 589.2 ($M + \text{H}$)⁺. HRMS-ESI (m/z) [$M +$
646 Na]⁺ calcd for $\text{C}_{31}\text{H}_{44}\text{N}_2\text{O}_7\text{NaS}$, 611.2769; found, 611.2767.
- 647 (1''S,1''R)-3-Hydroxy-N-(1''-{1'''-hydroxy-2''-[isobutyl-
648 (4-methoxy-benzenesulfonyl)amino]ethyl}hept-6''-enyl)-
649 2-pent-4''-enyl-enoxy-benzamide (21). Acid 11 was coupled
650 with amine 18 according to the general procedure for 20 to
651 give 21 (39 mg, 76%) as an oil: $[\alpha]_D^{25} -15.3$ (c 0.15, CHCl_3).
652 IR (neat): 3347, 1638, 1577, 1535, 1335 cm^{-1} . ^1H NMR (500
653 MHz, CDCl_3): δ 7.77 (d, 1 H, $J = 8.6$ Hz), 7.73 (dd, 1 H, $J =$
654 2.9, 11.9 Hz), 7.71 (dd, 1 H, $J = 2.0, 6.9$ Hz), 7.51 (dd, 1 H, $J =$
655 2.9, 6.7 Hz), 7.10 (m, 2 H), 6.98 (dd, 1 H, $J = 2.9, 11.8$ Hz),
656 6.97 (dd, 1 H, $J = 2.0, 6.9$ Hz), 5.89 (tdd, 1 H, $J = 6.7, 10.2,$
657 17.1 Hz), 5.77 (tdd, 1 H, $J = 6.7, 10.3, 17.0$ Hz), 5.71 (s, 1 H),
658 5.15 (ddd, 1 H, $J = 1.6, 3.2, 17.2$ Hz), 5.08 (dd, 1 H, $J = 1.5,$
659 10.1 Hz), 4.98 (ddd, 1 H, $J = 1.6, 3.4, 17.1$ Hz), 4.92 (m, 1 H),
660 4.09 (m, 1 H), 4.01 (m, 1 H), 3.93 (m, 2 H), 3.87 (s, 3 H), 3.78
661 (d, 1 H, $J = 3.2$ Hz), 3.21 (dd, 1 H, $J = 9.1, 15.1$ Hz), 3.01 (d,
662 1 H, $J = 1.9$ Hz), 2.98 (m, 1 H), 2.83 (dd, 1 H, $J = 6.6, 13.2$
663 Hz), 2.29 (q, 2 H, $J = 7.0$ Hz), 2.03 (m, 2 H), 1.98 (quint., 2 H,
664 $J = 7.0$ Hz), 1.85 (m, 1 H), 1.63 (m, 2 H), 1.45 (m, 2 H), 1.38
665 (m, 2 H), 0.91 (d, 3 H, $J = 6.6$ Hz), 0.86 (d, 3 H, $J = 6.6$ Hz).
666 ^{13}C NMR (125 MHz, CDCl_3): δ 165.8, 163.4, 149.6, 144.4,
667 139.1, 138.3, 130.3, 129.9, 127.1, 125.7, 122.9, 119.6, 116.3,
668 115.0, 114.8, 75.5, 73.5, 59.0, 56.0, 54.1, 53.2, 34.0, 30.7, 30.1,
669 29.4, 29.3, 27.6, 26.1, 20.5, 20.3. HRMS-ESI (m/z): ($M + \text{Na}$)⁺
670 calcd for $\text{C}_{32}\text{H}_{46}\text{N}_2\text{O}_7\text{NaS}$, 625.2934; found, 625.2923.
- 671 (2''R,15S)-N-[2''-Hydroxy-2''-(4-hydroxy-15-oxo-6,9,10-,
672 11,12,13,14,15-octahydro-5-oxa-14-aza-benzocyclotri-
673 decen-13-yl)ethyl]-N-isobutyl-4-methoxy-benzenesulfon-
674 amide (22). To a stirred solution of 19 (29.3 mg, 0.05 mmol)
675 in 20 mL of CH_2Cl_2 was added 4.2 mg (0.0051 mmol) of Grubbs'
676 catalyst. The solution was allowed to stir for 45 min under Ar
677 and then concentrated. Flash silica gel chromatography (40
678 to 45% EtOAc/hexanes) resulted in 22 (26.8 mg, 96%) as a
679 pale yellow foam as a mixture (5.5:1). IR (neat): 3341, 2953,
680 1635, 1575, 1538, 1463, 1333, 1260, 1152, 1091, 756 cm^{-1} . ^1H
681 NMR of trans diastereomer (400 MHz, CDCl_3): δ 8.13 (d, 1
682 H, $J = 9.2$ Hz), 7.66 (m, 2 H), 7.09 (d, 2 H, $J = 4.8$ Hz), 6.90
683 (d, 2 H, $J = 8.8$ Hz), 5.75 (m, 2 H), 5.35 (s, 1 H), 4.99 (dd, 1 H,
684 $J = 6.4, 11.2$ Hz), 4.27 (dd, 1 H, $J = 7.2, 11.2$ Hz), 4.00 (m, 1
685 H), 3.84 (s, 3 H), 3.81 (m, 1 H), 3.61 (d, 1 H, $J = 3.1$ Hz), 3.11
686 (dd, 1 H, $J = 8.7, 15.2$ Hz), 3.00 (m, 1 H), 2.89 (dd, 1 H, $J =$
687 8.2, 13.4 Hz), 2.80 (dd, 1 H, $J = 6.9, 13.4$ Hz), 2.25 (m, 1 H),
688 2.15 (m, 1 H), 1.79 (m, 1 H), 1.57–1.7 (m, 2 H), 1.56 (m, 3 H),
689 1.42 (m, 2 H), 0.87 (d, 3 H, $J = 6.6$ Hz), 0.81 (d, 3 H, $J = 6.7$
690 Hz). ^{13}C NMR (100 MHz, CDCl_3): δ 165.4, 162.9, 148.8, 145.3,
691 137.7, 129.7, 129.5, 126.3, 125.7, 124.6, 123.2, 120.0, 114.3,
692 73.4, 58.6, 55.6, 53.9, 52.9, 30.5, 27.1, 26.9, 24.0, 22.3, 20.0,
693 19.9. MS-ESI (m/z): 547.2 ($M + \text{H}$)⁺. HRMS-ESI (m/z) [$M +$
694 Na]⁺ calcd for $\text{C}_{28}\text{H}_{38}\text{N}_2\text{O}_7\text{NaS}$, 569.2299; found, 569.2297.
- 695 (2''R,14S)-N-[2''-Hydroxy-2''-(4-hydroxy-16-oxo-7,10,11-,
696 12,13,14,15,16-octahydro-6H-5-oxa-15-aza-benzocyclo-
697 radecen-14-yl)ethyl]-N-isobutyl-4-methoxy-benzene-
698 sulfonamide (23). To a stirring solution of 29 mg (0.046
699 mmol) of 20 in 25 mL of CH_2Cl_2 at 23 °C was added 3.6 mg
700 (0.0044 mmol) of Grubbs' catalyst. The solution was stirred
701 at 23 °C for 13.5 h and then concentrated. Purification by flash
702 silica gel chromatography (35–40% EtOAc/hexanes) resulted
703 in 23 (25 mg) as a white solid (89%) as a mixture of isomers
704 (10:1). IR (neat): 3340, 1634, 1577, 1530, 1332 cm^{-1} . ^1H NMR
705 of major isomer (500 MHz, CDCl_3): δ 7.69 (d, 2 H, $J = 8.9$
706 Hz), 7.51 (m, 2 H), 7.10 (m, 2 H), 6.94 (d, 2 H, $J = 8.9$ Hz), 706
5.78 (ddd, 1 H, $J = 5.5, 10.9, 14.9$ Hz), 5.50 (m, 1 H), 5.47 (s,
707 1 H), 4.16 (d, 1 H, $J = 4.7$ Hz), 3.99 (m, 2 H), 3.86 (s, 3 H),
708 3.81 (m, 1 H), 3.18 (dd, 1 H, $J = 2.8, 15.1$ Hz), 3.07 (dd, 1 H,
709 $J = 8.4, 15.1$ Hz), 2.91 (d, 2 H, $J = 7.6$ Hz), 2.59 (m, 1 H), 2.44
710 (m, 1 H), 2.19 (m, 2 H), 1.85 (m, 1 H), 1.74 (m, 1 H), 1.65–
711 1.42 (m, 5 H), 1.36 (m, 1 H), 0.86 (d, 3 H, $J = 6.6$ Hz), 0.84 (d,
712 3 H, $J = 6.7$ Hz). ^{13}C NMR (125 MHz, CDCl_3): δ 166.8, 163.3,
713 149.4, 144.8, 133.2, 130.8, 129.8, 128.5, 127.2, 125.6, 123.3,
714 120.0, 114.7, 75.9, 74.4, 58.4, 56.0, 55.1, 53.4, 34.2, 29.5, 27.3,
715 26.8, 25.3, 22.7, 20.5, 20.4.
- 716 (2''R,15S)-N-[2''-Hydroxy-2''-(4-hydroxy-17-oxo-6,7,8-,
717 11,12,13,14,15,16-decahydro-5-oxa-16-aza-benzocyclo-
718 pentadecen-15-yl)ethyl]isobutyl-4-methoxy-benzenesul-
719 fonamide (24). Acyclic diene 21 was subjected to the
720 conditions of olefin metathesis as described for 20 resulting
721 in 24 (29 mg, 89%) as a white solid (2:1 mixture). IR (neat):
722 3338, 1640, 1596, 1530 cm^{-1} . ^1H NMR of major isomer (400
723 MHz, CDCl_3): δ 7.71 (d, 2 H, $J = 8.9$ Hz), 7.37 (m, 1 H), 7.06
724 (m, 2 H), 6.95 (d, 2 H, $J = 8.8$ Hz), 5.78 (s, 1 H), 5.42 (m, 1 H),
725 5.25 (m, 1 H), 4.11 (m, 1H), 4.04 (m, 1 H), 3.86 (m, 4 H), 2.9
726 (d, 1 H, $J = 2.9$ Hz), 3.2 (dd, 1 H, $J = 9.0, 15.2$ Hz), 2.97 (m,
727 2 H), 2.81 (dd, 1 H, $J = 6.8, 15.0$ Hz), 2.30–2.00 (m, 3 H),
728 2.00–1.80 (m, 3 H), 1.70 (m, 1 H), 1.57 (m, 4 H), 1.4 (m, 2 H),
729 1.3 (m, 2 H), 0.91 (d, 3 H, $J = 6.7$ Hz), 0.85 (d, 3 H, $J = 6.7$
730 Hz). ^{13}C NMR (100 MHz, CDCl_3): δ 165.6, 163.0, 149.1, 144.4,
731 131.6, 130.5, 129.5, 126.6, 124.8, 121.8, 118.5, 114.4, 75.4, 74.4,
732 73.2, 58.7, 55.6, 53.9, 52.7, 30.9, 29.0, 27.6, 27.5, 27.2, 26.7,
733 24.0, 20.1, 19.9.
- 734 (1'S,1'R)-2,3-Dihydroxy-N-(1'-{1''-hydroxy-2''-[isobutyl-
735 (4-methoxy-benzenesulfonyl)amino]ethyl}octyl)-
736 benzamide (25). To a stirred solution of 22 (20.4 mg, 0.03
737 mmol), 2.8 mg of 10% Pd-C in 6 mL of MeOH was added,
738 and the resulting suspension was stirred at 23 °C under H_2
739 balloon for 3 h. The mixture was filtered through Celite and
740 concentrated. Flash silica gel chromatography (35% EtOAc/
741 hexanes) provided 25 (12.9 mg, 63%); mp 44–46 °C; $[\alpha]_D^{25} +3.6$
742 (c 0.30, CHCl_3). IR (neat): 3381, 2926, 1640, 1595, 1540, 1459,
743 1331, 1264, 1150, 1091, 1025, 806, 760 cm^{-1} . ^1H NMR (500
744 MHz, CDCl_3): δ 7.70 (dd, 1 H, $J = 3.0, 11.9$ Hz), 7.69 (dd, 1
745 H, $J = 2.0, 6.9$ Hz), 7.07 (d, 1 H, $J = 7.2$ Hz), 7.02 (dd, 1 H, $J =$
746 1.1, 8.2 Hz), 6.96 (dd, 1 H, $J = 1.6, 5.6$ Hz), 6.95 (dd, 1 H, $J =$
747 2.3, 11.8 Hz), 6.80 (m, 2 H), 5.80 (s, 1 H), 4.14 (qd, 1 H, $J =$
748 4.3, 13.7 Hz), 3.94 (td, 1 H, $J = 4.1, 11.6$ Hz), 3.86 (s, 3 H),
749 3.54 (d, 1 H, $J = 3.7$ Hz), 3.09 (m, 2 H), 2.92 (dd, 1 H, $J = 7.8,$
750 13.4 Hz), 2.87 (dd, 1 H, $J = 7.3, 13.4$ Hz), 1.86 (septet, 1 H, $J =$
751 6.8 Hz), 1.69 (m, 2 H), 1.25–1.30 (m, 9 H), 0.90 (d, 3 H, $J =$
752 6.3 Hz), 0.89 (d, 3 H, $J = 6.3$ Hz), 0.86 (t, 3 H, $J = 6.9$ Hz). ^{13}C
753 NMR (125 MHz, CDCl_3): δ 170.6, 163.5, 149.6, 146.3, 130.0,
754 129.9, 119.2, 118.7, 116.6, 114.8, 114.1, 73.5, 59.3, 56.0, 53.9,
755 53.3, 32.2, 29.8, 29.7, 29.6, 27.7, 26.6, 23.0, 20.5, 20.4, 14.5.
756 MS-ESI (m/z): 573.3 ($M + \text{Na}$)⁺. HRMS-ESI (m/z) [$M + \text{Na}$]⁺
757 calcd for $\text{C}_{28}\text{H}_{42}\text{N}_2\text{O}_7\text{NaS}$, 573.2613; found, 573.2610.
- 758 (2''R,14S)-N-[2''-Hydroxy-2''-(4-hydroxy-16-oxo-7,8,9-,
759 10,11,12,13,14,15,16-decahydro-6H-5-oxa-15-aza-benzocyclo-
760 clotradecen-14-yl)ethyl]-N-isobutyl-4-methoxy-ben-
761 zenesulfonamide (26). A mixture of 23 (21 mg, 0.037 mmol)
762 and 2.7 mg of 10% Pd-C in 10 mL of MeOH was stirred at 23
763 °C under H_2 balloon for 4 h. The mixture was then filtered
764 through Celite and concentrated. Purification by flash silica
765 gel chromatography (40% EtOAc/hexanes) provided 26 (14 mg,
766 69%) as a white solid; mp 63–65 °C. $[\alpha]_D^{25} +12.9$ (c 0.35,
767 CHCl_3). IR (neat): 3350, 1637, 1596, 1531, 1331 cm^{-1} . ^1H NMR
768 (500 MHz, CDCl_3): δ 7.69 (dd, 1 H, $J = 2.9, 11.7$ Hz), 7.68
769 (dd, 1 H, $J = 1.8, 7.0$ Hz), 7.38 (dd, 1 H, $J = 3.6, 5.9$ Hz), 7.28
770 (d, 1 H, $J = 7.3$ Hz), 7.09 (m, 2 H), 6.94 (dd, 2 H, $J = 2.9, 11.7$
771 Hz), 5.79 (m, 1 H), 4.16–4.10 (m, 2 H), 3.86 (m, 4 H), 3.72 (d,
772 1 H, $J = 3.2$ Hz), 3.14 (dd, 1 H, $J = 8.7, 15.2$ Hz), 3.04 (dd, 1
773 H, $J = 3.0, 15.2$ Hz), 2.91 (dd, 1 H, $J = 8.1, 13.4$ Hz), 2.83 (dd,
774 1 H, $J = 7.0, 13.4$ Hz), 1.92 (m, 2 H), 1.82 (septet, 1 H, $J = 6.9$
775 Hz), 1.68 (m, 2 H), 1.57–1.37 (m, 9 H), 1.25 (m, 2 H), 0.87 (d,
776 3 H, $J = 7.1$ Hz), 0.83 (d, 3 H, $J = 6.6$ Hz). ^{13}C NMR (125
777 MHz, CDCl_3): δ 166.7, 163.4, 149.6, 144.5, 130.3, 129.9, 128.1,
778 125.5, 122.6, 119.4, 114.7, 75.6, 74.1, 59.0, 56.0, 54.0, 53.2, 28.5,
779

780 28.3, 27.5, 26.7, 24.4, 24.2, 23.6, 23.2, 20.5, 20.3. HRMS-ESI
781 (*m/z*) [M + Na]⁺ calcd for C₃₀H₄₄N₂O₇NaS, 599.2767; found,
782 599.2792.

783 (2''*R*,15*S*)-*N*-[2''-Hydroxy-2''-(4-hydroxy-17-oxo-6,7,8,9-,
784 10,11,12,13,14,15,16,17-dodecahydro-5-oxa-16-aza-benzo-
785 cyclopentadecen-15-yl)ethyl]-*N*-isobutyl-4-methoxybenzo-
786 zenesulfonamide (27). Hydrogenation of 24 following the
787 procedure for 26 resulted in 27 (13 mg, 78%) as a white solid;
788 mp 69–72.5 °C. [α]_D²³ +9.3 (c 0.49, CHCl₃). IR (neat): 3343,
789 1638, 1596, 1577, 1531, 1332 cm⁻¹. ¹H NMR (500 MHz,
790 CDCl₃): δ 7.69 (m, 2 H), 7.28 (d, 1 H, *J* = 2.2 Hz), 7.18 (dd, 1
791 H, *J* = 8.9 Hz), 7.06 (m, 2 H), 6.94 (d, 2 H, *J* = 8.9 Hz), 5.90
792 (s, 1 H), 4.13 (m, 2 H), 3.96–3.87 (m, 2 H), 3.85 (s, 3 H), 3.84
793 (d, 1 H, *J* = 3.3 Hz), 3.12 (dd, 1 H, *J* = 8.4, 15.2 Hz), 3.05 (dd,
794 1 H, *J* = 3.1, 15.2 Hz), 2.92 (dd, 1 H, *J* = 8.1, 13.4 Hz), 2.86
795 (dd, 1 H, *J* = 7.0, 13.3 Hz), 1.90 (m, 2 H), 1.84 (m, 1 H), 1.73–
796 1.66 (m, 3 H), 1.50–1.36 (m, 1 H), 0.89 (d, 3 H, *J* = 6.6 Hz),
797 0.85 (d, 3 H, *J* = 6.6 Hz). ¹³C NMR (125 MHz, CDCl₃): δ 167.1,
798 163.4, 149.7, 144.4, 130.3, 129.9, 128.6, 125.2, 121.8, 119.0,
799 114.7, 75.1, 73.7, 59.1, 56.0, 54.1, 53.1, 29.4, 28.1, 27.6, 26.6,
800 26.0, 25.3, 24.6, 24.1, 23.5, 20.5, 20.3. MS-ESI (*m/z*): 599.3
801 [M + Na]⁺. HRMS-ESI (*m/z*) [M + Na]⁺ calcd for C₃₀H₄₄N₂O₇-
802 NaS, 599.2769; found, 599.2767.

803 (1''*S*,1''*R*)-2-But-3'-enyloxy-3-hydroxy-*N*-(1''-{1''-hy-
804 droxy-2''-[isobutyl-(4-methoxybenzenesulfonyl)amino]-
805 ethyl}hex-5''-enyl)benzamide (29). Acid 10 was coupled
806 with amine 28 according to the general procedure for 19 to
807 give 29 in 45% yield as an oil: [α]_D²³ -4.4 (c 3.1, CHCl₃). IR
808 (neat): 3344, 2958, 1632, 1577, 1534, 1497, 1462, 1333, 1260,
809 1152, 1091, 1023, 995, 807, 757 cm⁻¹. ¹H NMR (400 MHz,
810 CDCl₃): δ 7.72 (d, 2 H, *J* = 8.8 Hz), 7.48 (dd, 1 H, *J* = 2.2, 7.3
811 Hz), 7.10 (m, 2 H), 6.97 (d, 2 H, *J* = 8.8 Hz), 5.96 (tdd, 1 H, *J*
812 = 6.9, 10.2, 17.2 Hz), 5.82 (s, 1 H), 5.77 (tdd, 1 H, *J* = 6.8,
813 10.2, 16.9 Hz), 5.31 (m, 1 H), 4.98 (m, 1 H), 4.09 (m, 2 H), 3.94
814 (m, 2 H), 3.87 (s, 3 H), 3.79 (d, 1 H, *J* = 3.1 Hz), 3.21 (dd, 1 H,
815 *J* = 9.2, 15.2 Hz), 2.99 (m, 2 H), 2.82 (dd, 1 H, *J* = 6.6, 13.3
816 Hz), 2.57 (m, 2 H), 2.09 (m, 2 H), 1.86 (m, 1 H), 1.62–1.70 (m,
817 2 H), 1.52–1.58 (m, 2 H), 1.43–1.52 (m, 3 H), 0.92 (d, 3 H, *J*
818 = 6.6 Hz), 0.86 (d, 3 H, *J* = 6.6 Hz). ¹³C NMR (125 MHz,
819 CDCl₃): δ 165.8, 163.5, 149.6, 144.3, 138.7, 134.6, 130.3, 129.9,
820 127.2, 125.8, 122.6, 119.7, 119.5, 115.4, 114.8, 74.8, 73.5, 59.1,
821 56.0, 54.1, 53.0, 34.6, 34.0, 28.7, 27.7, 25.8, 20.5, 20.3. MS-
822 ESI (*m/z*): 597.2 [M + Na]⁺.

823 (2''*R*,13*S*)-*N*-[2''-Hydroxy-2''-(4-hydroxy-15-oxo-6,7,8,9-,
824 10,11,12,13,14,15-decahydro-5-oxa-14-aza-benzocyclo-
825 tridecen-13-yl)ethyl]-*N*-isobutyl-4-methoxybenzenesulfon-
826 amide (30). Acyclic diene 29 (42 mg) was cyclized under the
827 conditions of olefin metathesis as described for 19 to give the
828 corresponding cyclic olefin (37.7 mg, 75%, 1.9:1 mixture) as
829 as a foam. IR (neat): 3347, 2958, 1633, 1596, 1577, 1535, 1497,
830 1463, 1332, 1290, 1260, 1152, 1091, 1025, 998, 807, 755 cm⁻¹;
831 major isomer. ¹H NMR (500 MHz, CDCl₃): δ 7.84 (d, 1 H, *J* =
832 6.9 Hz), 7.67 (d, 2 H, *J* = 8.9 Hz), 7.51 (dd, 1 H, *J* = 2.0, 7.6
833 Hz), 7.02 (m, 2 H), 6.91 (d, 2 H, *J* = 8.9 Hz), 6.52 (s, 1 H), 5.60
834 (dd, 1 H, *J* = 6.12, 15.7 Hz), 5.55 (dd, 1 H, *J* = 5.5, 15.6 Hz),
835 4.26 (m, 2 H), 4.16 (m, 1 H), 3.95 (m, 1 H), 3.84 (s, 3 H), 3.15
836 (dd, 1 H, *J* = 3.2, 15.2 Hz), 3.00 (dd, 1 H, *J* = 8.4, 15.2 Hz),
837 2.90 (m, 2 H), 2.44 (m, 1 H), 2.35 (m, 1 H), 1.87 (m, 2 H), 1.81
838 (m, 1 H), 1.75 (m, 1 H), 1.67 (m, 2 H), 1.53 (m, 1 H), 0.83 (dd,
839 6 H, *J* = 6.7, 8.7 Hz). ¹³C NMR (125 MHz, CDCl₃): δ 166.8,
840 163.3, 149.5, 144.6, 134.0, 130.5, 129.9, 128.4, 127.0, 124.6,
841 123.3, 120.5, 114.7, 74.1, 73.8, 58.7, 56.0, 54.1, 53.6, 32.4, 31.5,
842 27.6, 27.4, 24.4, 20.4, 20.4.

843 Hydrogenation of above olefin mixture for 1 h following the
844 procedure for 26 resulted in saturated macrocycle 30 as a
845 colorless solid (15.7 mg) in 71% yield; mp 74–75.5; [α]_D²³ +29.9
846 (c 0.73, CHCl₃). IR (neat): 3348, 2951, 2931, 1635, 1596, 1577,
847 1534, 1497, 1464, 1332, 1288, 1260, 1151, 1091, 1025, 996, 807,
848 755 cm⁻¹. ¹H NMR (500 MHz, CDCl₃): δ 7.66 (d, 2 H, *J* = 8.9
849 Hz), 7.27 (m, 2 H), 7.04 (m, 2 H), 6.92 (d, 2 H, *J* = 8.9 Hz),
850 5.95 (s, 1 H), 4.12 (m, 2 H), 3.91 (m, 1 H), 3.85 (bs, 4 H), 3.08
851 (d, 2 H, *J* = 4.2 Hz), 2.86 (d, 2 H, *J* = 7.5 Hz), 1.93 (m, 1 H),
852 1.86 (m, 1 H), 1.79 (pentet, 1 H, *J* = 6.8 Hz), 1.69 (m, 4 H),
853 1.58 (m, 2 H), 1.48 (m, 3 H), 1.42 (m, 2 H), 0.86 (d, 3 H, *J* =

6.6 Hz), 0.82 (d, 3 H, *J* = 6.6 Hz). ¹³C NMR (125 MHz, 854
CDCl₃): δ 167.1, 163.4, 149.4, 144.4, 130.2, 129.9, 128.5, 125.1, 855
122.2, 119.3, 114.7, 74.1, 73.4, 59.0, 56.0, 54.2, 52.7, 29.5, 27.8, 856
27.5, 26.3, 24.1, 21.5, 21.4, 20.4, 20.3. HRMS-ESI (*m/z*) [M + 857
K]⁺ calcd for C₂₉H₄₂N₂O₇NaS, 585.2610; found, 585.2591. 858

859 (1''*S*,1''*R*)-*N*-(1''-{2''-Benzo[1''',3''']dioxole-5''-sulfo-
860 nyl}isobutyl-aminol-1''-hydroxyl-ethyl}hept-6''-enyl)-2-
861 but-3'-enyloxy-3-hydroxy-benzamide (32). Acid 10 and
862 amine 31 were coupled according to the method used for 19
863 to give 32 (38 mg, 57%) as a yellow oil: [α]_D²³ -12.2 (c 0.18,
864 CHCl₃). IR (neat): 3355, 1638, 1576, 1536, 1331 cm⁻¹. ¹H NMR
865 (500 MHz, CDCl₃): δ 7.68 (d, 1 H, *J* = 8.6 Hz), 7.48 (dd, 1 H,
866 *J* = 2.2, 7.3 Hz), 7.34 (dd, 1 H, *J* = 1.8, 6.4 Hz), 7.20 (d, 1 H,
867 *J* = 1.8 Hz), 7.10 (m, 2 H), 6.88 (d, 1 H, *J* = 8.2 Hz), 6.09 (s,
868 2 H), 5.96 (tdd, 1 H, *J* = 6.9, 10.3, 17.1 Hz), 5.77 (m, 2 H),
869 5.33 (dd, 1 H, *J* = 1.4, 17.2 Hz), 5.29 (d, 1 H, *J* = 10.3 Hz),
870 4.98 (m, 1 H), 4.92 (d, 1 H, *J* = 10.2 Hz), 4.09 (m, 2 H), 3.97
871 (m, 2 H), 3.79 (d, 1 H, *J* = 3.29 Hz), 3.79 (d, 1 H, *J* = 3.3 Hz),
872 3.21 (dd, 1 H, *J* = 9.0, 15.1 Hz), 3.04 (d, 1 H, *J* = 2.6 Hz), 3.00
873 (m, 1 H), 2.85 (dd, 1 H, *J* = 6.7, 13.4 Hz), 2.57 (m, 2 H), 2.04
874 (dd, 2 H, *J* = 6.8, 11.9 Hz), 1.87 (ddd, 1 H, *J* = 6.7, 6.7, 14.8
875 Hz), 1.64 (m, 2 H), 1.45 (m, 2 H), 1.39 (m, 1 H), 0.92 (d, 3 H,
876 *J* = 6.6 Hz), 0.87 (d, 3 H, *J* = 6.6 Hz). ¹³C NMR (100 MHz,
877 CDCl₃): δ 165.5, 151.5, 149.2, 148.3, 143.9, 138.6, 134.1, 131.6,
878 126.8, 125.4, 123.1, 122.2, 119.3, 119.1, 114.6, 108.4, 107.5,
879 102.4, 74.4, 73.1, 58.7, 53.6, 52.9, 34.1, 33.6, 29.7, 28.8, 27.2,
880 25.7, 20.1, 19.8. MS-ESI (*m/z*): 625.2 [M + Na]⁺. HRMS-ESI
881 (*m/z*) [M + Na]⁺ calcd for C₃₁H₄₂N₂O₈NaS, 625.2562; found,
882 625.2560.

883 (2''*R*,14*S*)-Benzo[1''',3''']dioxole-5''-sulfonic Acid [2''-Hy-
884 droxy-2''-(4-hydroxy-16-oxo-7,8,9,10,11,12,13,14,15,16-
885 decahydro-6*H*-5-oxa-15-aza-benzocyclohexadecen-14-
886 yl)ethyl]isobutyl-amide (33). Acyclic diene 32 (31 mg) was
887 subjected to the conditions of olefin metathesis as described
888 for 22 to provide the corresponding cyclic olefin (29 mg, 9:1
889 mixture) in 95% yield. IR (neat): 3350, 1634, 1576, 1530, 1330
890 cm⁻¹. ¹H NMR of major (trans) diastereomer (500 MHz,
891 CDCl₃): δ 7.53 (m, 1 H), 7.31 (m, 1 H), 7.18 (m, 1 H), 7.11 (m,
892 2 H), 6.83 (d, 1 H, *J* = 8.2 Hz), 6.08 (s, 2 H), 5.8 (m, 1 H), 5.5
893 (m, 2 H), 4.22 (d, 1 H, *J* = 4.9 Hz), 3.98 (m, 3 H), 3.9 (m, 1 H),
894 3.21 (m, 1 H), 3.07 (dd, 1 H, *J* = 8.5, 15.2 Hz), 2.93 (m, 2 H),
895 2.60 (m, 1 H), 2.50 0.85 (d, 3 H, *J* = 6.8 Hz). ¹³C NMR (125
896 MHz, CDCl₃): δ 166.8, 151.7, 149.4, 148.6, 144.8, 133.1, 132.6,
897 129.8, 128.5, 127.1, 125.6, 123.4, 123.3, 120.1, 108.7, 108.0,
898 102.7, 74.4, 58.4, 55.3, 53.3, 34.2, 29.5, 27.3, 26.9, 25.3, 22.7,
899 20.5, 20.3.

900 Hydrogenation of above olefin mixture according to the
901 procedure for 26 afforded 33 (20 mg, 91%) as a white solid;
902 mp 64–65.5 °C; [α]_D²³ +15.5 (c 0.62, CHCl₃). IR (neat): 3348,
903 1637, 1532, 1329 cm⁻¹. ¹H NMR (500 MHz, CDCl₃): δ 7.38
904 (dd, 1 H, *J* = 3.1, 6.5 Hz), 7.31 (m, 2 H), 7.17 (d, 1 H, *J* = 1.7
905 Hz), 7.07 (m, 2 H), 6.83 (d, 1 H, *J* = 8.2 Hz), 6.07 (s, 2 H), 5.91
906 (s, 1 H), 4.20–4.04 (m, 2 H), 3.90–3.80 (m, 2 H), 3.76 (d, 1 H,
907 *J* = 3.1 Hz), 3.16–3.07 (m, 2 H), 2.92 (dd, 1 H, *J* = 5.3, 13.4
908 Hz), 2.85 (dd, 1 H, *J* = 7.0, 13.4 Hz), 1.91 (m, 1H), 1.80 (m, 1
909 H), 1.69 (m, 3 H), 1.51–1.41 (m, 8 H), 1.26 (m, 2 H), 0.88 (d,
910 3 H, *J* = 6.7 Hz), 2.3 (m, 2 H), 1.87 (m, 1 H), 1.73 (m, 1 H), 1.5
911 (m, 5 H), 0.87 (d, 3 H, *J* = 6.7 Hz), 6.6), 0.83 (d, 3 H, *J* = 6.6
912 Hz). ¹³C (125 MHz, CDCl₃): δ 166.8, 151.9, 149.7, 148.7, 144.5,
913 132.0, 128.0, 125.5, 123.5, 122.6, 119.5, 108.8, 107.9, 102.7,
914 75.5, 74.1, 59.0, 54.0, 53.3, 28.5, 28.3, 27.5, 26.6, 24.4, 24.2,
915 23.5, 23.2, 20.5, 20.3. HRMS-ESI (*m/z*) [M + Na]⁺ calcd for
916 C₂₉H₄₀N₂O₈Na, 599.2403; found, 599.2378.

917 **Antiviral Assay.** The activity of designated compounds
918 against HIV-1LAI was determined as previously described.^{3a}
919 Briefly, MT-2 cells (2 × 10⁶/well) were exposed to 100 50%
920 tissue culture infectious doses (TCID₅₀s) of HIV-1LAI in the
921 presence of various concentrations of an agent, examined in
922 96 well microculture plates, and incubated at 37 °C for 7 days
923 (final volume: 200 μL/well). After the medium was removed
924 from each well, 10 μL of 3-(4,5-dimethylthiazol-2-yl)-2,5-
925 diphenyltetrazolium bromide (MTT) solution (7.5 mg/mL) in
926 phosphate-buffered saline was added to each well in the
927 plate, followed by incubation at 37 °C for 2 h. After incubation,

928 to dissolve the formazan crystals, 100 μ L of acidified 2-pro-
929 panol containing 4% (v/v) Triton X-100 was added to each well
930 and the optical density (570 nm) was measured in a microplate
931 reader (Vmax; Molecular Devices, Sunnyvale, CA). All assays
932 were conducted in duplicate.

933 **Acknowledgment.** Financial support of this work
934 by the National Institutes of Health (Grant GM 53386
935 to A.K.G.) and a grant for the promotion of AIDS
936 research from the Ministry of Health, Labor and Wel-
937 fare (Kosei-Rodosho) of Japan (to H.M.) is gratefully
938 acknowledged.

939 **Supporting Information Available:** HRMS and HPLC
940 data for compounds 19–22, 25–27, 30, 32, and 33. This
941 material is available free of charge via the Internet at [http://](http://pubs.acs.org)
942 pubs.acs.org.

943 References

- 944 (1) (a) Sepkowitz, K. A. AIDS—The first 20 years. *N. Engl. J. Med.*
945 **2001**, *344*, 1764–1772. (b) Cihlar, T.; Bischofberger, N. Recent
946 developments in antiretroviral therapies. *Ann. Rev. Med. Chem.*
947 **2000**, *35*, 177–89. (c) Flexner, C. W. Pharmacology of drug
948 interactions of HIV protease inhibitors. In *Protease Inhibitors*
949 *in AIDS Therapy*; Ogden, R. C., Flexner, C. W., Eds.; Marcel
950 Dekker: New York, 2001; pp 139–160.
- 951 (2) (a) Ghosh, A. K.; Shin, D. W.; Swanson, L.; Krishnan, K.; Cho,
952 H.; Hussain, K. A.; Walters, D. E.; Holland, L.; Buthod, J.
953 Structure-based design of non-peptide HIV protease inhibitors.
954 *Pharmaco* **2001**, *56*, 29–32. (b) Ghosh, A. K.; Kincaid, J. F.; Cho,
955 W.; Walters, D. E.; Krishnan, K.; Hussain, K. A.; Koo, Y.; Cho,
956 H.; Rudall, C.; Holland, L.; Buthod, J. Potent HIV protease
957 inhibitors incorporating high affinity P₂-ligands and (R)-
958 (hydroxyethylamino)sulfonamide isostere. *Bioorg. Med. Chem.*
959 *Lett.* **1998**, *8*, 687–90.
- 960 (3) (a) Koh, Y.; Nakata, H.; Maeda, K.; Ogata, H.; Bilcer, G.;
961 Devasamudram, T.; Kincaid, J. F.; Boross, P.; Wang, Y.-F.; Tie,
962 Y.; Volarath, P.; Gaddis, L.; Harrison, R. W.; Weber, I. T.; Ghosh,
963 A. K.; Mitsuya, H. A novel bis-tetrahydrofuranylethane-
964 containing non-peptide protease inhibitor (PI) UIC-94017 (TMC-
965 114) potent against multi-PI-resistant HIV in vitro. *Antimicrob.*
966 *Agents Chemother.* **2003**, *47*, 3123–29. (b) Yoshimura, K.; Kato,
967 R.; Kavlick, M. F.; Nguyen, A.; Maroun, V.; Maeda, K.; Hussain,
968 K. A.; Ghosh, A. K.; Gulnik, S. V.; Erickson, J. W.; Mitsuya, H.
969 UIC-94003: A potent protease inhibitor (PI) that inhibits multi-
970 PI-resistant HIV-1 replication in vitro. *J. Virol.* **2002**, *76*, 1349–
971 1358.
- 972 (4) (a) Ghosh, A. K.; Leshchenko, S.; Noetzel, M. Stereoselective
973 photochemical 1,3-dioxalene addition to α,β -unsaturated- γ -lactone:
974 Synthesis of bis-tetrahydrofuran ligand for HIV protease
975 inhibitor UIC-94-017 (TMC-114). *J. Org. Chem.* **2004**, *69*, 7822–
976 29. (b) Ghosh, A. K.; Chen, Y. Synthesis and optical resolution
977 of high affinity P₂-ligands for HIV-1 protease inhibitors. *Tetra-*
978 *hedron Lett.* **1995**, *36*, 505. (c) Ghosh, A. K.; Kincaid, J. F.;
979 Walters, D. E.; Chen, Y.; Chaudhuri, N. C.; Thompson, W. J.;
980 Culberson, C.; Fitzgerald, P. M. D.; Lee, H. Y.; McKee, S. P.;
981 Munson, P. M.; Duong, T. T.; Darke, P. L.; Zugay, J. A.; Schleif,
982 W. A.; Axel, M. G.; Lin, J.; Huff, J. R. Nonpeptidic P₂-ligands
983 for HIV protease inhibitors: Structure-based design, synthesis
984 and biological evaluation. *J. Med. Chem.* **1996**, *39*, 3278–90.
- 985 (5) Tie, Y.; Boross, P. I.; Wang, Y.-F.; Gaddis, L.; Hussain, K. K.;
986 Leshchenko, S.; Ghosh, A. K.; Louis, J. M.; Harrison, R. W.;

- Weber, I. T. High-resolution crystal structures of HIV-1 protease 987
with a potent non-peptide inhibitor (UIC-94017) active against 988
multi-drug resistant clinical strains. *J. Mol. Biol.* **2004**, *338*, 989
341–352.
- (6) De Meyers, S.; Peeters, M. Conference on Retroviruses and 991
Opportunistic Infections (11th CROI), February 8–11, 2004, San 992
Francisco, CA; Abstracts 533 and 620. 993
- (7) (a) Mitsunobu, O. The use of diethyl azodicarboxylate and 994
triphenylphosphine in synthesis and transformation of natural 995
products. *Synthesis* **1981**, 1–28. 996
- (8) Gao, Y.; Hanson, R. M.; Klunder, J. M.; Ko, S. Y.; Masamune, 997
H.; Sharpless, K. B. Catalytic asymmetric epoxidation and 998
kinetic resolution: Modified procedures including in situ de- 999
rivatization. *J. Am. Chem. Soc.* **1987**, *109*, 5765–5780. 1000
- (9) Caron, M.; Carlier, P. R.; Sharpless, K. B. Regioselective azide 1001
opening of 2,3-epoxy alcohols by [Ti(O-*i*-Pr)₂(N₃)₂]: Synthesis of 1002
 α -amino acids. *J. Org. Chem.* **1988**, *53*, 5185–5187. 1003
- (10) Ghosh, A. K.; McKee, S. P.; Lee, H. Y.; Thompson, W. J. A facile 1004
and enantiospecific synthesis of 2(S)- and 2(R)-[1'(S)-azido-2- 1005
phenylethyl] oxirane. *J. Chem. Soc. Chem. Commun.* **1992**, 273– 1006
274. 1007
- (11) Evans, B. E.; Rittle, K. E.; Homnick, C. F.; Springer, J. P.; 1008
Hirshfield, J.; Veber, D. F. A stereocontrolled synthesis of 1009
hydroxyethylene dipeptide isosteres using novel chiral, amino 1010
alkyl epoxides and γ -(aminoalkyl) γ -lactones. *J. Org. Chem.* 1011
1985, *50*, 4615–4625. 1012
- (12) Grubbs, R. H.; Chang, S. Recent advances in olefin metathesis 1013
and its application in organic synthesis. *Tetrahedron* **1998**, *54*, 1014
4413–4450. 1015
- (13) Bergmann, E.; Heimhold, H. Rearrangement of allyl ethers in 1016
the purine series, with some remarks on the hydrogenation of 1017
allyl ethers. *J. Chem. Soc.* **1935**, 1365–1367. 1018
- (14) Chung, S.-K. Selective reduction of mono- and disubstituted 1019
olefins by sodium borohydride and cobalt (II). *J. Org. Chem.* 1020
1979, *44*, 1014–1016. 1021
- (15) This arylsulfonfyl chloride was prepared by bromination of 1,2- 1022
methyleneedioxybenzene with NBS¹⁶ and halogen–metal ex- 1023
change with ⁿBuLi in hexane at –78 °C followed by reaction of 1024
the lithium salt with SO₂Cl₂. 1025
- (16) Gensler, W. J.; Stouffer, J. E. Compounds related to podophyl- 1026
lotoxin. IX. 3,4-Methyleneedioxyphenyllithium. *J. Org. Chem.* 1027
1958, *23*, 908. 1028
- (17) Toth, M. V.; Marshall, G. R. A simple, continuous fluorometric 1029
assay for HIV protease. *Int. J. Pept. Protein Res.* **1990**, *36*, 544– 1030
550. 1031
- (18) Roberts, N. A.; Martin, J. A.; Kinchington, D.; Broadhurst, A. 1032
V.; Craig, J. C.; Duncan, I. B.; Galpin, S. A.; Handa, B. K.; Kay, 1033
J.; Krohn, A.; Lambert, R. W.; Merrett, J. H.; Mills, J. S.; Parkes, 1034
K. E. B.; Redshaw, S.; Ritchie, A. J.; Taylor, D. L.; Thomas, G. 1035
J.; Machin, P. J. Rational design of peptide-based HIV proteinase 1036
inhibitors. *Science* **1990**, *248*, 358–361. 1037
- (19) (a) Noble, S.; Goa, K. L. Amprenavir: A review of its clinical 1038
potential in patients with HIV infection. *Drugs* **2000**, *60*, 1383– 1039
1410. (b) Kim, E. E.; Baker, C. T.; Dwyer, M. D.; Murcko, M. A.; 1040
Rao, B. G.; Tung, R. D.; Navia, M. A. Crystal structure of HIV-1 1041
protease in complex with VX-478, a potent and orally bioavail- 1042
able inhibitor of the enzyme. *J. Am. Chem. Soc.* **1995**, *117*, 1181– 1043
1182. 1044
- (20) Weiner, S. J.; Kollman, P. A.; Nguyen, D. T.; Case, D. A. An all 1045
atom force field for simulations of proteins and nucleic acids. *J.* 1046
Comput. Chem. **1986**, *7*, 230–252. 1047
- (21) To analyze the protein–ligand interactions of this class of 1048
inhibitors, crystallographic studies of the HIV-1 protease com- 1049
plex of inhibitor **26** are being attempted. 1050

JM050019I

1051

Spontaneous recovery of hemoglobin and neutrophil levels in Japanese patients on a long-term Combivir[®] containing regimen

Shuzo Matsushita^{a,d,*}, Kazuhisa Yoshimura^{a,d}, Tetsuya Kimura^a, Asako Kamihira^b,
Misao Takano^c, Kenichiro Eto^d, Takuma Shirasaka^b, Hiroaki Mitsuya^d, Shinichi Oka^c

^a Division of Clinical Retrovirology and Infectious Diseases, Center for AIDS Research, Kumamoto University, 2-2-1 Honjo, Kumamoto 860-0811, Japan

^b Department of Immunological and Infectious Diseases, Osaka National Hospital, Osaka 540-0006, Japan

^c AIDS Clinical Center, International Medical Center of Japan, Tokyo 162-8655, Japan

^d Department of Infectious Diseases, Kumamoto University School of Medicine, Kumamoto 860-8556, Japan

Received 11 August 2004; accepted 3 November 2004

Abstract

Objective: In order to evaluate long-term toxicity of Combivir, we retrospectively reviewed clinical records of HIV-1 infected cases under treatment with Combivir-containing regimen and we analyzed the clinical data compared to other NRTIs-containing regimens.

Study design: A total of 55 patients who were on Combivir and 39 on a control regimen were examined.

Results: After starting treatment with Combivir-containing regimens viral load and CD4⁺ T-cell count improved as well as the control group. Rates of adverse events in Combivir group and ZDV (400 mg/day) + 3TC group were 50.9% (28/55) and 60% (12/20), respectively. Some of these Japanese patients who started Combivir regimen as a first-line HAART (primary Combivir group) showed some decrease in hemoglobin levels or neutrophil counts within 6 months. However, a significant recovery of these indices of hematological toxicities occurred in patients who continued the regimen for 18–24 months.

Conclusion: Our findings suggest that the safety of 600 mg of ZDV is similar to 400 mg/day of ZDV and the existence of mechanisms that compensate for anemia and for the neutropenia associated with long-term use of Combivir.

© 2004 Elsevier B.V. All rights reserved.

Keywords: Combivir; Zidovudine; Lamivudine; Hemoglobin; Neutrophil; Long-term treatment

1. Introduction

Prognosis of HIV infections dramatically improved after introduction of highly active anti-retroviral therapy (HAART). However, the occurrence of adverse events and drug resistance during long-term use of anti-retrovirals are now big issues (Yeni et al., 2002; Dieleman et al., 2002). Present HAART also has a problem to maintain a high adherence because of the pill burden and patients' quality of life is affected. Combivir[®] is a fixed dose combination tablet containing zidovudine (ZDV) and lamivudine (3TC) (Eron

et al., 2000). Each tablet contains 300 mg of ZDV and 150 mg of 3TC and has been widely used as a nucleoside reverse transcriptase inhibitor (NRTI) component of HAART against HIV-1 infection.

HIV infection and AIDS are known to be associated with a significant hematological toxicity, including anemia, neutropenia, and thrombocytopenia (Moses et al., 1998). In addition, studies with zidovudine have shown that this drug may compound the hematological toxicity of HIV and lead to an independent development of anemia and neutropenia (Wilde and Langtry, 1993). Consistent with these observations, the incidence of anemia or neutropenia in mildly or asymptomatic adults treated with zidovudine was between 1.1% and 9.7%, whereas in adults with AIDS or the AIDS related complex it ranged from 15% to as high as 61% (Wilde

* Corresponding author. Tel.: +81 96 373 6536; fax: +81 96 373 6537.
E-mail address: shuzo@kaiju.medic.kumamoto-u.ac.jp
(S. Matsushita).